

Ag⁺-Specific Pyridine Podands: Effects of Ligand Geometry and Stereochemically Controlled Substitution on Cation Complexation and Transport Functions

Hiroshi Tsukube,^{*,†} Satoshi Shinoda,[†] Jun'ichi Uenishi,^{*,‡} Takao Hiraoka,[‡]
Takahiro Imakoga,[‡] and Osamu Yonemitsu[‡]

Department of Chemistry, Graduate School of Science, Osaka City University, Sugimoto, Sumiyoshi-ku, Osaka 558-8585, Japan, and Department of Chemistry, Faculty of Science, Okayama University of Science, Ridai-cho, Okayama 700-0005, Japan

Received November 18, 1997

A new series of acyclic podands was designed so that three pyridine moieties cooperatively bind a guest Ag⁺. Liquid–liquid extraction, NMR binding, and computer calculation experiments reveal that podands with three pyridine donors in a proper geometry exhibit a perfect Ag⁺ specificity. They selectively extracted Ag⁺ in the presence of equimolar Pb²⁺, Cu²⁺, Ni²⁺, Co²⁺, and Zn²⁺. Introduction of two chiral centers close to the pyridine binding sites surprisingly influences the Ag⁺-binding ability of the podand. Fourteen new pyridine podands were evaluated as carriers in a liquid membrane transport system. A combination of ligand geometry and stereocontrolled substitution provides excellent Ag⁺-specific transport.

Synthetic podands are a family of linear multidentate ligands which includes acyclic polyethers. They generally form complexes with smaller stability constants than those of corresponding macrocyclic complexes and thus are usually regarded as poor ligands.¹ In contrast, there are many excellent podands in nature. For example, naturally occurring polyether antibiotics, such as monensin and lasalocid, selectively bind several metal cations and effectively transport them across a biomembrane.² Although they have acyclic podand-type structures, geometrical and stereochemical arrangements of cation-ligating donors in the acyclic skeleton provide specific cation-binding properties. Lasalocid typically has a salicylate anion and several oxygen donor atoms located in the pseudocyclic skeleton. It has 10 asymmetric carbons and exhibits higher cation binding ability than nonbiological stereoisomers.³ Synthetic podands have advantages over these biological podands, in terms of facile synthesis and versatility of molecular structure. Since the number of synthetic podands showing specific binding abilities is still limited,¹ there are many things to learn from biological podand systems.⁴

Here, we present a new series of specific podands based on geometrical and stereochemical optimizations of the ligand structure.⁵ We systematically prepare Ag⁺-specific podands which have three pyridine donors as binding sites and two asymmetric centers close to them (Chart

1). Ag⁺-selective binders are of great utility in ¹¹¹Ag-based radioimmunotherapy and photographic techniques, as well as in the separation of Ag⁺ from natural source or wastewater.⁶ Ag⁺ usually has a linear bidentate coordination mode but occasionally forms tridentate or highly coordinated complexes.⁷ We chose pyridine nitrogen atoms as soft donor groups and placed three pyridine rings in the acyclic skeleton to form a selective and stable Ag⁺ complex. The newly designed pyridine podands were found to exhibit perfect Ag⁺ selectivity *via* 1:1 complexation. We further introduced two CH₃ substituents close to the pyridine binding sites in a stereochemically controlled fashion and noted remarkable differences in extraction and transport abilities between certain stereoisomers. The stereocontrolled substitution enhanced the Ag⁺-binding ability of the podand. Thus, a proper combination of ligand geometry and stereospecific substitution led to the development of Ag⁺-selective podands.

Results and Discussion

Design of Pyridine Podands. Molecular design of new specific ligands has usually included empirical "trial-and-error" exercises, but computational methods are expected to provide a rational basis for their design.⁸ We performed modeling experiments to optimize the structures of Ag⁺ complexes with pyridine podands. Computer

[†] Osaka City University.

[‡] Okayama University of Science.

(1) (a) Tsukube, H. In *Crown Ethers and Analogous Compounds*; Hiraoka, M., Ed.; Elsevier: New York, 1992; pp 100–197. (b) Gokel, G. W.; Murillo, O. In *Molecular Recognition: Receptors for Cationic Guests*; Comprehensive Supramolecular Chemistry, Vol. 1; Pergamon Press: New York, 1996; pp 1–33.

(2) (a) Tsukube, H. In *Cation Binding by Macrocycles*; Inoue, Y., Gokel, G. W., Eds.; Marcel Dekker: New York, 1991; pp 497–522. (b) Dobler, M. In *Molecular Recognition: Receptors for Cationic Guests*; Comprehensive Supramolecular Chemistry, Vol. 1; Pergamon Press: New York, 1996; pp 267–313.

(3) Still, W. C.; Hauck, P.; Kempt, D. *Tetrahedron Lett.* **1987**, *28*, 2817–2820.

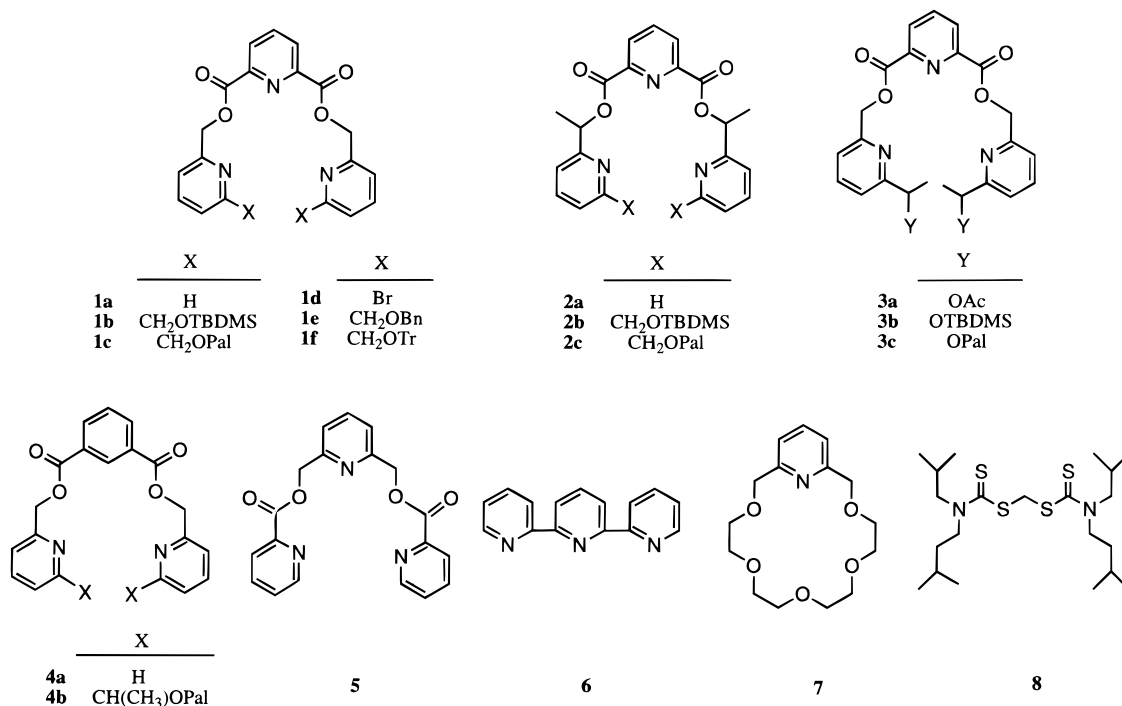
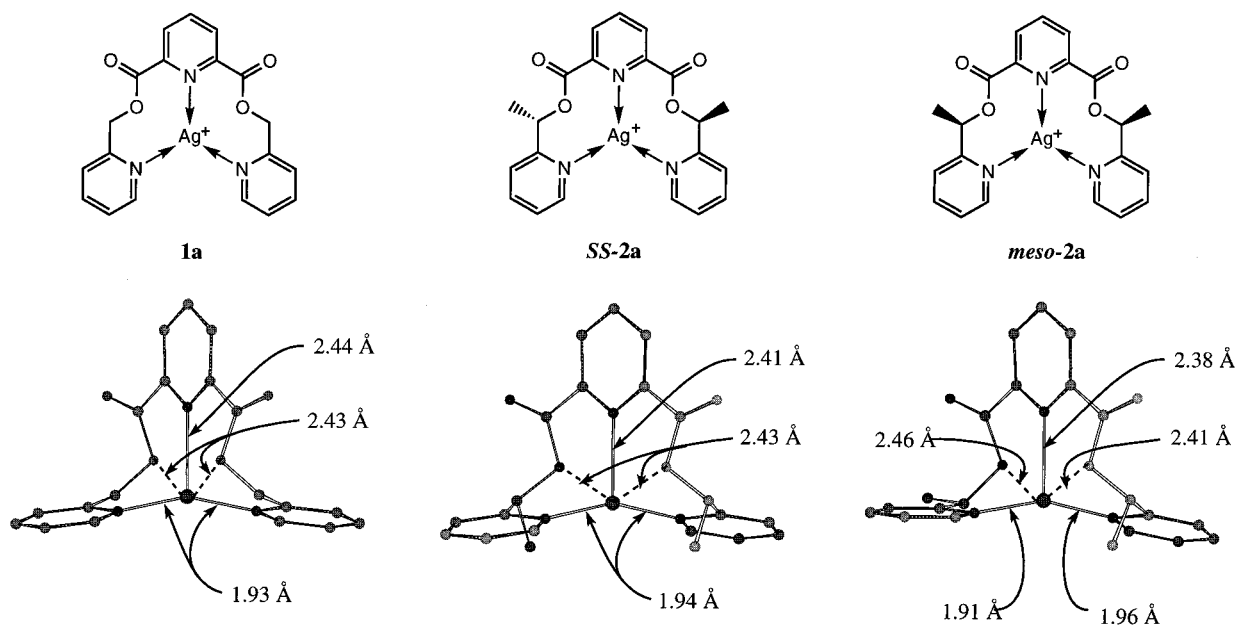
(4) (a) Tsukube, H.; Sohmiya, H. *Supramol. Chem.* **1993**, *1*, 297–304. (b) Lindoy, J. F. *Coord. Chem. Rev.* **1996**, *148*, 349–368.

(5) Preliminary communications: (a) Tsukube, H.; Uenishi, J.; Kojima, N.; Yonemitsu, O. *Tetrahedron Lett.* **1995**, *36*, 2257–2260. (b) Tsukube, H.; Uenishi, J.; Hiraoka, T.; Yonemitsu, O. *Enantiomer* **1997**, *2*, 281–285.

(6) (a) Parker, D. *Chem. Soc. Rev.* **1990**, *19*, 271–291. (b) Bakker, W. I. I.; Verboom, W.; Reinhoudt, D. N. *J. Chem. Soc., Chem. Commun.* **1994**, 71–72.

(7) (a) Kang, H. C.; Hanson, A. W.; Eaton, B.; Boekelheide, V. J. *Am. Chem. Soc.* **1985**, *107*, 1979–1985. (b) Heitzer, F. R.; Hopf, H.; Jones, P. G.; Bubenitschek, P.; Lehne, V. *J. Org. Chem.* **1993**, *58*, 2781–2784.

(8) (a) Wipff, G.; Troxler, L. In *Computational Approaches in Supramolecular Chemistry*; Wipff, G., Ed.; Kluwer Academic Press: The Netherlands, 1994; pp 319–348. (b) Tsukube, H. *Coord. Chem. Rev.* **1996**, *148*, 1–17.

Chart 1. Tridentate Pyridine Podands and Related Compounds^a^a Pal = CO(CH₂)₁₄CH₃.**Figure 1.** Optimized structures of pyridine podand-Ag⁺ complexes.

modeling and energy calculations were performed using Spartan SGI version 4.0.1 (*ab initio*, STO-3G). In the calculations, the effects of counteranion and the tail group were neglected. Figure 1 illustrates the optimized structures of Ag⁺ complexes with three kinds of pyridine podands: **1a**, **SS-2a**, and **meso-2a**. These have three pyridine donors in the acyclic skeletons, but the orientation of the pyridine rings is slightly altered in the Ag⁺ complexes. For podand **1a**, Ag⁺ is very nicely coordinated by three pyridine nitrogen atoms, indicating that the three nitrogen donors are arranged so as to converge on the guest Ag⁺. The calculated distances between the nitrogen atoms of terminal pyridines and Ag⁺ are 1.93 Å, while that between the nitrogen atom of central

pyridine and Ag⁺ is 2.44 Å. Both are comparable to those observed in solid-state structures for other types of pyridine-Ag⁺ complexes.⁹ Although the oxygen atoms of the ester moieties are located near the Ag⁺, their lone pair electrons did not point to it. Thus, the three pyridine nitrogens were indicated as the potential binding sites. For chiral **SS-2a** and its *meso*-form, there are interesting differences in the calculated structures and energies of their Ag⁺ complexes. **SS-2a** has a symmetrical arrangement of the three pyridine rings for binding of Ag⁺, and the Ag⁺ is equally coordinated by the two terminal

(9) Engelhardt, L. M.; Pakawatchai, C.; White, A. H.; Healy, P. C. *J. Chem. Soc., Dalton Trans.* **1985**, 117-123.

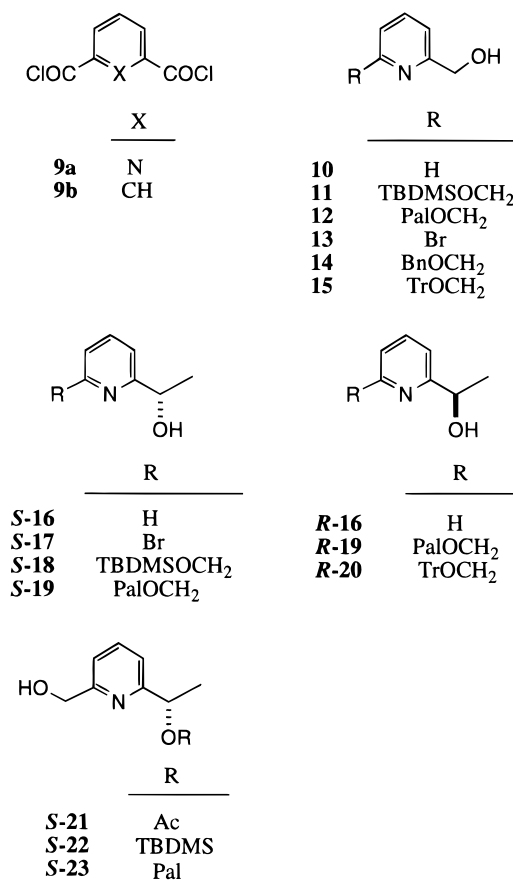
pyridine rings. Distances between the two nitrogen atoms and Ag⁺ are the same (1.94 Å). In contrast, **meso-2a** forms a different type of Ag⁺ complex in which two terminal pyridine nitrogen atoms coordinate with Ag⁺ in an asymmetrical fashion. Distances between nitrogen atoms of terminal pyridines and Ag⁺ are calculated to be 1.91 and 1.96 Å, respectively. Thus, introduction of two CH₃ substituents significantly modifies the coordination mode of Ag⁺. These structural features also influence the stability of the Ag⁺ complex. In energy calculations the stabilized energy of the **SS-2a** complex is larger by 3.46 kcal/mol than that of the **meso-2a** complex. Thus, proper stereocontrolled substitution of the pyridine podand is calculated to enhance Ag⁺-binding ability.

Synthesis of Pyridine Podands. Three kinds of pyridine podands were prepared: **1a–f** have three pyridine rings in the podand skeletons; **2a–c** have two additional CH₃ substituents in the middle of the chain; and **3a–c** also have two substituents on the tails (see Chart 1). We obtained stereoisomers having the *SS*- and *meso*-configurations of podands **2a–c**, while *meso*-isomers of podands **3a–c** were not prepared. Because these podands had stereocontrolled substituents as well as three pyridine donors, we compared their cation-binding properties to determine the effects of stereocontrolled substitution. Different types of podands **4a,b** and **5** were also synthesized for comparison. Podands **4a,b** have one benzene and two pyridine rings, and **5** has different linkages between the pyridine units from those in podands **1–4**. Compounds **6** and **7** are common pyridine ligands for heavy and transition-metal cations, while **8** was reported to be a Ag⁺-specific ionophore.¹⁰

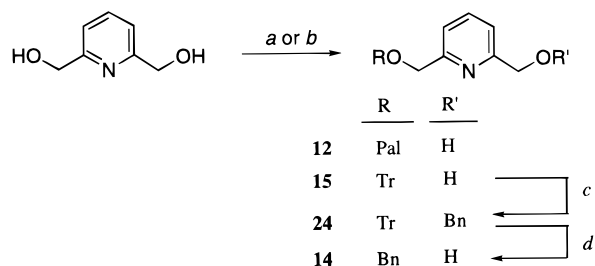
We developed a new synthetic route to the optically pure pyridine precursors for preparation of podands **2–4** (Chart 2), because the reported synthetic reactions of chiral or bifunctional pyridine derivatives included reaction sequences and procedures for scale-up which were too complicated.¹¹ Our synthetic strategy was to resolve the enantiomers of the pyridine building block *via* enzymatic reaction. Lipase-catalyzed acetylation provided ready access to multigram quantities of the optically pure pyridineethanol derivatives.¹² Kinetic resolution of racemic pyridineethanol **18** was typically performed by *Candida antarctica* lipase with vinyl acetate in diisopropyl ether. We obtained both enantiomers with 99% ee or better in good yields.

For the synthesis of pyridine podands **1–4**, a variety of achiral and chiral pyridine alcohols were required. Their structures are depicted in Chart 2, and syntheses are shown in Schemes 1–3. Scheme 1 describes the preparation of unsymmetrically substituted pyridinemethanols **12**, **14**, and **15**. Palmitoylation of one of the hydroxyl groups of 2,6-pyridinedimethanol with palmitoyl chloride in the presence of triethylamine gave **12** in 70% yield, while monotrityl ether **15** was obtained by trity-

Chart 2. Pyridineethanols for Synthesis of Pyridine Podands



Scheme 1^a



^a Reagents and conditions: (a) PalCl, Et₃N, THF–CH₂Cl₂ (1:1), rt; (b) TrCl, Et₃N, THF–CH₂Cl₂ (10:1), rt; (c) NaH, PhCH₂Br, THF–DMF (2:5), rt; (d) K₂CO₃, MeOH–CH₂Cl₂ (3:2), rt.

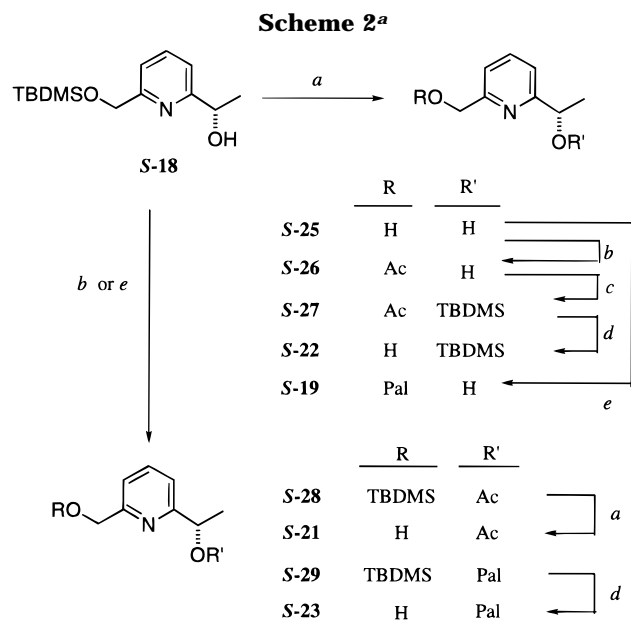
lation in 64% yield. Monobenzyl ether **14** was derived from **15** *via* **24** in the following steps: (i) benzyl ether formation of the other hydroxyl group with benzyl bromide and NaH (93%) and (ii) deprotection of the trityl group with hydrochloric acid (96%).

Scheme 2 shows the synthetic routes to optically active pyridineethanols **S-19**, **S-21**, **S-22**, and **S-23** from **S-18**, which was obtained in an enantiomerically pure form by *C. antarctica* lipase-catalyzed acetylation of racemic **18**.¹² Desilylation of **S-18** with Bu₄NF gave **S-25** in 96% yield. Palmitoylation of the primary alcohol of **S-25** with palmitoyl chloride afforded **S-19** in 94% yield. Acetylation of **S-25** with acetic anhydride, silylation of the remaining secondary alcohol with TBDMSCl, and deprotection of the acetate provided **S-22** in 90% yield *via* **S-26** and **S-27** in three steps. Pyridinemethanols **S-21** and **S-23** were derived from **S-18** in two steps: acetylation of **S-18** gave **S-28** in 94% yield, which upon treatment

(10) (a) Izatt, R. M.; Pawlak, K.; Bradshaw, J. S.; Bruening, R. I. *Chem. Rev.* **1991**, *91*, 1721–2085. (b) Lerch, M.; Reitter, E.; Simon, W.; Pretsch, E. *Anal. Chem.* **1994**, *66*, 1713–1717.

(11) Some optically active pyridine derivatives have been prepared as the chiral auxiliary: (a) Soai, K.; Niwa, S.; Kobayashi, T. *J. Chem. Soc., Chem. Commun.* **1987**, 801–802. (b) Bolm, C.; Eward, M.; Zehnder, M.; Neuburger, M. A. *Chem. Ber.* **1992**, *125*, 453–458. (c) Nishiyama, H.; Yamaguchi, S.; Park, S. B.; Itoh, K. *Tetrahedron: Asymmetry* **1993**, *4*, 143–150.

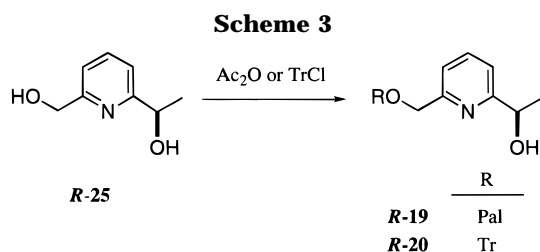
(12) (a) Uenishi, J.; Nishiwaki, K.; Hata, S.; Nakamura, K. *Tetrahedron Lett.* **1994**, *35*, 7973–7976. (b) Uenishi, J.; Hiraoka, T.; Hata, S.; Nishiwaki, K.; Yonemitsu, O.; Nakamura, K.; Tsukube, H. *J. Org. Chem.* **1998**, *63*, 2481–2487.



^a Reagents and conditions: (a) Bu₄NF, THF, rt; (b) Ac₂O, Et₃N, CH₂Cl₂, rt; (c) TBDMSCl, imidazole, DMF, rt; (d) K₂CO₃, MeOH, rt; (e) PalCl, Et₃N, CH₂Cl₂, rt.

with Bu₄NF gave **S-21** in 97% yield. In the same reaction sequence, palmitoylation of **S-18** followed by desilylation afforded **S-23** in 75% yield.

As shown in Scheme 3, **R-19** and **R-20** were prepared by acetylation and tritylation of **R-25** in 95% and 78% yields, respectively.



These pyridine alcohols were coupled with 2,6-pyridinedicarbonyl dichloride (**9a**) or 1,3-benzenedicarbonyl dichloride (**9b**) to afford pyridine podands **1a–f**, chiral **2a–c**, chiral **3a–c**, and chiral **4a,b** (Scheme 4). The results are summarized in Table 1. The yields were generally excellent, and the obtained podands were mostly solids.

Scheme 4. Synthesis of Pyridine Podands

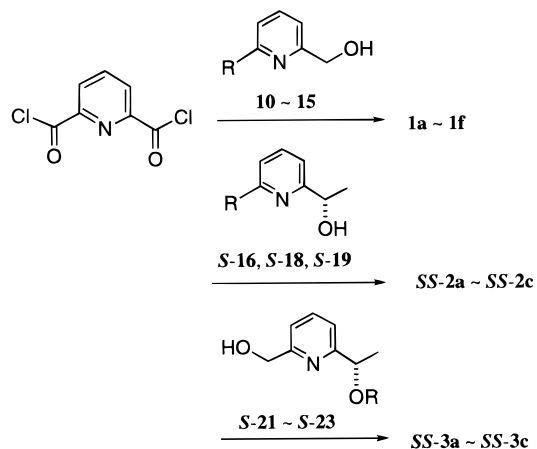
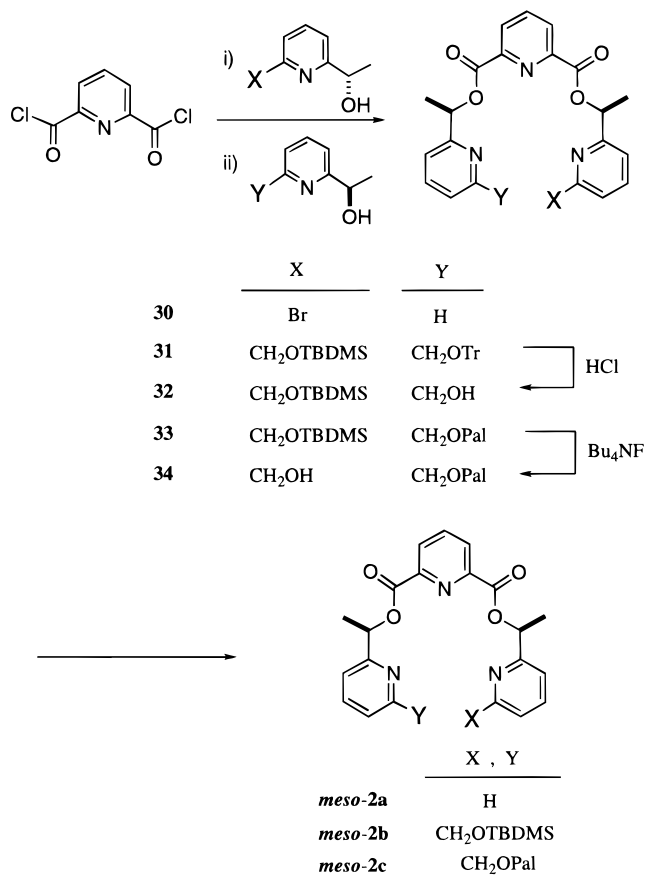


Table 1. Coupling Reaction of Pyridineethanols with 2,6-Pyridinedicarbonyl and 1,3-Benzenedicarbonyl Dichlorides

entry	acid chloride	pyridineethanol	product	yield (%)
1	9a	10	1a	75
2	9a	11	1b	92
3	9a	12	1c	70
4	9a	13	1d	87
5	9a	14	1e	72
6	9a	15	1f	95
7	9a	S-16	SS-2a	80
8	9a	S-18	SS-2b	87
9	9a	S-19	SS-2c	95
10	9a	S-21	SS-3a	88
11	9a	S-22	SS-3b	94
12	9a	S-23	SS-3c	90
13	9b	10	4a	86
14	9b	S-23	SS-4b	86

meso-2a, **meso-2b**, and **meso-2c**, in contrast, were synthesized by stepwise coupling with the *S*-alcohol and then the *R*-alcohol in one pot (Scheme 5). Successive

Scheme 5. Synthesis of meso-Pyridine Podands



additions of equivalent amounts of **S-17** and **R-16** to **9a** produced unsymmetric podand **30** in 64% yield together with symmetric pyridine podand **2a** in 9% yield. Hydrogenolysis of bromide **30** with Bu₃SnH gave exclusively **meso-2a** in 60% yield. Podand **meso-2b** was assembled from the three components, **S-18**, **R-20**, and **9a**, in the same manner described for the synthesis of **meso-2a**. The coupling provided unsymmetrical podand **31** in 36% yield together with **SS-2b** in 11% yield. Deprotection of the trityl group with ZnBr₂ followed by silylation of the resulting hydroxyl group with TBDMSCl afforded **meso-2b** in 81% yield in two steps. Using the same reaction sequence, **meso-2c** was obtained from reaction of **S-18**

and **R-19** with **9a**. The three components were coupled in 68% yield giving **33**, which afforded *meso-2c* through **34** in 30% yield in two steps. Podands **3a–c** with a *SS*-configuration were prepared from the corresponding optically pure pyridineethanols, while statistical mixtures of *SS*-, *RR*-, and *meso*-isomers were derived from racemic pyridineethanols. Since *SS*-, *RR*-, and *meso*-isomers of each podand were not separable by any chromatographic technique or recrystallization, independent synthesis of the chiral and *meso*-podands was necessary. The obtained chiral podands **2a–c** and **3a–c** had sufficient optical purities to allow for evaluation of the stereochemical effect on the cation complexation, and their cation-binding behaviors were compared with those of corresponding *meso*-isomers and statistical mixtures of *SS*-, *RR*-, and *SR*-isomers.

Cation Extraction. Cation-binding abilities of the newly prepared pyridine podands were assessed by solvent extraction of heavy and transition-metal cations.¹³ A total of 14 pyridine podands **1–5** were examined together with the three reference ligands **6–8**. The extraction ability was estimated on the basis of partition of metal perchlorates between methylene chloride and an aqueous solution. Typical results for the competitive extraction experiments are summarized in Table 2. These results were obtained for extraction of an aqueous mixture of equimolar Ag⁺, Pb²⁺, Cu²⁺, Ni²⁺, Co²⁺, and Zn²⁺.

The pyridine podands exhibit perfect Ag⁺ selectivity in the presence of equimolar Pb²⁺, Cu²⁺, Ni²⁺, Co²⁺, and Zn²⁺, and some of them extracted Ag⁺ more efficiently than the common Ag⁺-specific ligands **7** and **8** (see Table 2). For a series of podands **1a–f**, ether and silyl ether derivatives **1b,e**, and **f** exhibited higher extractabilities for Ag⁺ than ester derivative **1c**. Since unsubstituted and bromide derivatives **1a,d** produced considerable amounts of insoluble materials under the extraction conditions, the nature of the tail group (X or Y in Chart 1) is judged to greatly influence extraction behavior of the podand. Podand **4b** was also employed but gave negligible extraction for all the metal cations. Since this podand has one benzene and two pyridine rings, cooperativity of the three pyridine rings is clearly demonstrated. When the aqueous phase contained a mixture of Ag⁺, Li⁺, Na⁺, and K⁺, podands with three pyridine rings were also found to extract Ag⁺ selectively. Thus, the present type of pyridine podands exhibits highly Ag⁺-selective extraction.

Podands **2a–c** and **3a–c** which have additional substituents exhibited Ag⁺-specific extraction, but their two CH₃ substituents introduced close to the pyridine binding sites affected Ag⁺ extraction efficiency. There were marked differences in the extraction percentages between the stereoisomers of **2a–c**, whereas only slight effects were observed with podands **3a–c**. *K*_{ex} values were estimated for podands **2a–c**. These were defined as [podand-Ag⁺]_{org}/[Ag⁺]_{aq} × [podand]_{org} and calculated from

(13) Recent examples of pyridine-containing receptors: (a) Westmark, P. R.; Gardiner, S. J.; Smith, B. D. *J. Am. Chem. Soc.* **1996**, *118*, 11093–11100. (b) Hasenknopf, B.; Lehn, J. M.; Kneisel, B. O.; Baum, G.; Fenske, D. *Angew. Chem., Int. Ed. Engl.* **1996**, *35*, 1838–1840. (c) Habata, Y.; Bradshaw, J. S.; Zhang, X. X.; Izatt, R. M. *J. Am. Chem. Soc.* **1997**, *119*, 7145–7146. (d) Kelly, T. R.; Lee, Y. J.; Mears, R. J. *J. Org. Chem.* **1997**, *62*, 2774–2781. (e) Santos, O.; Lajmi, A. R.; Canary, J. W. *Tetrahedron Lett.* **1997**, *38*, 4383–4386. (f) Takeuchi, M.; Yamamoto, M.; Shinkai, S. *J. Chem. Soc., Chem. Commun.* **1997**, 1731–1732.

Table 2. Cation-Extraction Properties of Pyridine Podands

podand	extraction percentage ^a					
	Ag ⁺	Pb ²⁺	Cu ²⁺	Ni ²⁺	Co ²⁺	Zn ²⁺
1a	<i>b</i>	<i>b</i>	<i>b</i>	<i>b</i>	<i>b</i>	<i>b</i>
1b	80	<3	<3	<3	<3	<3
1c^c	52	<3	<3	<3	<3	<3
1d	<i>b</i>	<i>b</i>	<i>b</i>	<i>b</i>	<i>b</i>	<i>b</i>
1e	97	<3	<3	<3	<3	<3
1f	80	<3	<3	<3	<3	<3
SS-2a^c	96	<3	<3	<3	<3	<3
meso-2a	76	<3	<3	<3	<3	<3
2a^d	79	<3	<3	<3	<3	<3
SS-2b	90	<3	<3	<3	<3	<3
meso-2b	77	<3	<3	<3	<3	<3
2b^d	72	<3	<3	<3	<3	<3
SS-2c	73	<3	<3	<3	<3	<3
meso-2c	47	<3	<3	<3	<3	<3
2c^d	60	<3	<3	<3	<3	<3
SS-3a	57	<3	<3	<3	<3	<3
3a^d	54	<3	<3	<3	<3	<3
SS-3b	79	<3	<3	<3	<3	<3
3b^d	73	<3	<3	<3	<3	<3
SS-3c	59	<3	<3	<3	<3	<3
3c^d	62	<3	<3	<3	<3	<3
SS-4b	<3	<3	<3	<3	<3	<3
4b^d	<3	<3	<3	<3	<3	<3
5	<i>b</i>	<i>b</i>	<i>b</i>	<i>b</i>	<i>b</i>	<i>b</i>
6^c	<3	<3	21	<3	<3	<3
7	62	<3	<3	<3	<3	<3
8	67	5	<3	<3	<3	<3

^a Aqueous layer: AgClO₄, Pb(ClO₄)₂, Cu(ClO₄)₂, Ni(ClO₄)₂, Co(ClO₄)₂, and Zn(ClO₄)₂, 0.030 mmol each in 3 mL of H₂O. Organic phase: podand, 0.030 mmol in 3 mL of CH₂Cl₂. ^b Insoluble material appeared. ^c Turbidity appeared. ^d A statistical mixture of *SS*-, *RR*-, and *meso*-isomers (1:1:2).

the concentrations of Ag⁺ in the aqueous phase prior to and after extraction. Their values are *K*_{ex} = 50 100 for **SS-2a**, 1300 for **meso-2a**, 8600 for **SS-2b**, 1500 for **meso-2b**, 1000 for **SS-2c**, and 170 for **meso-2c**. Interestingly, **SS-2b** has a 5.7 times larger *K*_{ex} value than **meso-2b**. Since the latter had a similar *K*_{ex} value to that of unsubstituted podand **1b** (*K*_{ex} = 2000), stereocontrolled substitution remarkably enhanced the Ag⁺ extraction ability of the pyridine podand. Much larger enhancement (ca. 38.5 times) was observed between the stereoisomers of podand **2a**, although the corresponding unsubstituted podand **1a** gave precipitate under the same conditions. Podands **3a–c** also have two CH₃ substituents on the tail groups. However, their stereoisomers showed almost the same Ag⁺ extraction efficiencies, which were also similar to those of corresponding unsubstituted podands **1a–c** (see Table 2). Therefore, both the location and stereochemistry of the introduced substituents are found to be important factors in determining Ag⁺ extraction efficiency in these pyridine podand systems.¹⁴ Terpyridine **6**, which is known to be a strong chelating reagent for several metal cations, extracted Cu²⁺ moderately under the employed conditions. Thus, the geometrical arrangement of three pyridine rings in the podand skeleton creates a unique cation recognition profile.

NMR Studies of Ag⁺ Binding. Further detailed information on the Ag⁺-binding behaviors of the pyridine

(14) The effect of stereochemically controlled substitution on the metal cation-binding property of a ligand was reported in a few cases: (a) Erickson, S. D.; Still, W. C. *Tetrahedron Lett.* **1990**, *31*, 4253–4256. (b) Sasaki, S.; Naito, H.; Maruta, K.; Kawahara, E.; Maeda, M. *Tetrahedron Lett.* **1994**, *35*, 3337–3340. (c) Shibutani, Y.; Mino, S.; Long, S. S.; Moriuchi-Kawakami, T.; Yakabe, K.; Shono, T. *Chem. Lett.* **1997**, 49–50.

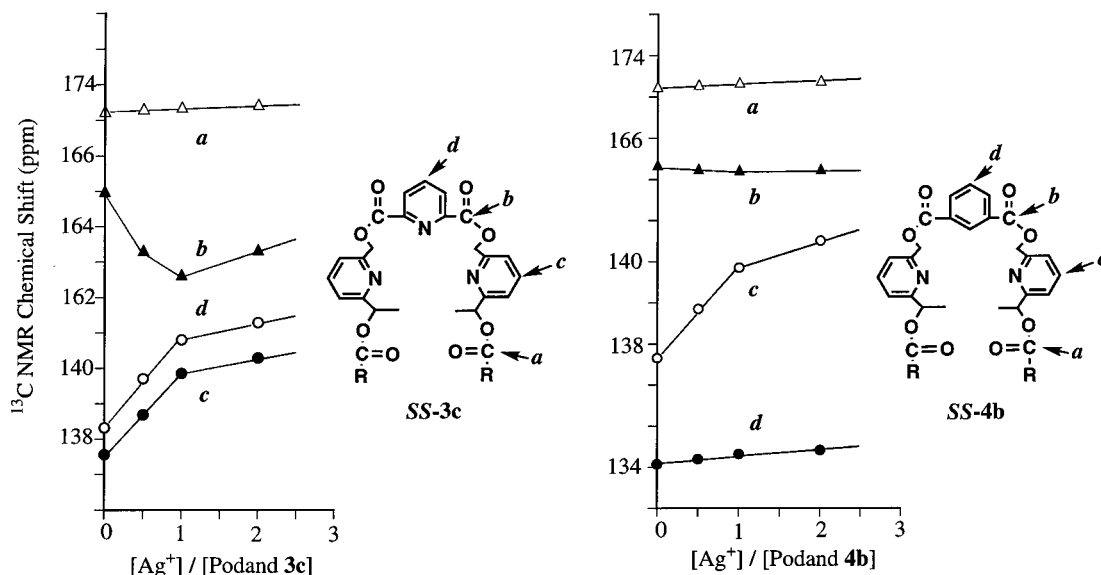


Figure 2. Ag⁺ ion-induced ¹³C NMR spectral changes of podands **3c** and **4b**.

podands was obtained using NMR spectroscopy. Figure 2 illustrates the Ag⁺-induced changes in the ¹³C NMR chemical shifts of the selected carbon signals in **SS-3c** and **SS-4b**, which have three and two pyridine rings, respectively. The addition of AgClO₄ to a solution (CDCl₃–CH₃OH, 4:1) of each podand caused significant and continuous spectral changes. Since these titration curves had clear breaks at [Ag⁺]/[podand] = 1.0, 1:1 complexation was confirmed in both podand systems. When podand **SS-3c** was employed, significant shifts were observed in the signals for carbons of the three pyridine rings. Since the ester carbon signal on the tail shifted only slightly, the three pyridine rings predominantly and cooperatively bound the Ag⁺. Podand **SS-4b** is suggested to form a 1:1 Ag⁺ complex in a different fashion. Signals for the two pyridine rings shifted, although those for benzene and ester moieties showed little change. Thus, podand **4b** formed a bidentate complex with Ag⁺, while podand **3c** wrapped around the Ag⁺ *via* cooperativity of the three pyridine donors. ¹H NMR binding experiments provided parallel results to those in ¹³C NMR experiments: cooperative binding of the pyridine rings and 1:1 complexation. Since these experimental results are consistent with those of the computer calculations (see Figure 1), a proper arrangement of the three pyridine donors is shown to be effective in accommodating Ag⁺ and offering high Ag⁺ specificity.

Cation Transport across a Liquid Membrane. Results of the cation-binding and extraction experiments suggest that the present type of pyridine podands has potential as effective carriers of Ag⁺. Competitive cation-transport experiments were carried out in a CH₂Cl₂ liquid membrane system.¹³ Table 3 summarizes the transport results for various pyridine podands when a mixture of AgClO₄, Pb(ClO₄)₂, Cu(ClO₄)₂, Ni(ClO₄)₂, Co(ClO₄)₂, and Zn(ClO₄)₂ was employed as the aqueous source phase. Pyridine podands **1a–f**, **2a–c**, and **3a–c** exhibit perfect Ag⁺ selectivity in the transport process as well as in the extraction, while bidentate podand **4b** was an inefficient carrier. Podands **3a–c** showed higher Ag⁺-transport efficiencies than the corresponding podands **1a–c** and **2a–c**. Podand **SS-3c** exhibited a 2-fold higher transport rate than corresponding podand **SS-2c**,

Table 3. Cation-Transport Properties of Pyridine Podands

podand	transport rate 10 ⁶ (mol/h) ^a					
	Ag ⁺	Pb ²⁺	Cu ²⁺	Ni ²⁺	Co ²⁺	Zn ²⁺
1a	0.6	<0.1	<0.1	<0.1	<0.1	<0.1
1b	4.8	<0.1	<0.1	<0.1	<0.1	<0.1
1d^b	2.3	<0.1	<0.1	<0.1	<0.1	<0.1
1e	1.5	<0.1	<0.1	<0.1	<0.1	<0.1
1f	3.1	<0.1	<0.1	<0.1	<0.1	<0.1
SS-2a	1.9	<0.1	<0.1	<0.1	<0.1	<0.1
meso-2a	2.1	<0.1	<0.1	<0.1	<0.1	<0.1
2a^c	2.6	<0.1	<0.1	<0.1	<0.1	<0.1
SS-2b	2.0	<0.1	<0.1	<0.1	<0.1	<0.1
meso-2b	2.8	<0.1	<0.1	<0.1	<0.1	<0.1
2b^c	2.6	<0.1	<0.1	<0.1	<0.1	<0.1
SS-2c	2.8	<0.1	<0.1	<0.1	<0.1	<0.1
meso-2c	5.7	<0.1	<0.1	<0.1	<0.1	<0.1
2c^c	3.8	<0.1	<0.1	<0.1	<0.1	<0.1
SS-3a	4.6	<0.1	<0.1	<0.1	<0.1	<0.1
3a^c	7.1	<0.1	<0.1	<0.1	<0.1	<0.1
SS-3b	3.9	<0.1	<0.1	<0.1	<0.1	<0.1
3b^c	5.5	<0.1	<0.1	<0.1	<0.1	<0.1
SS-3c	5.9	<0.1	<0.1	<0.1	<0.1	<0.1
3c^c	5.3	<0.1	<0.1	<0.1	<0.1	<0.1
SS-4b	0.2	<0.1	<0.1	<0.1	<0.1	<0.1
4b^c	0.2	<0.1	<0.1	<0.1	<0.1	<0.1
5	1.0	<0.1	<0.1	<0.1	<0.1	<0.1
6	<0.1	<0.1	0.2	<0.1	<0.1	<0.1
7	4.6	<0.1	<0.1	<0.1	<0.1	<0.1
8	5.1	<0.1	<0.1	<0.1	<0.1	<0.1

^a Aqueous source phase: AgClO₄, Pb(ClO₄)₂, Cu(ClO₄)₂, Ni(ClO₄)₂, Co(ClO₄)₂, and Zn(ClO₄)₂, 0.50 mmol each in 5 mL of H₂O. Membrane: podand, 0.0186 mmol in 12 mL of CH₂Cl₂. Aqueous receiving phase: 5 mL of H₂O. ^b Insoluble material appeared. ^c A statistical mixture of *SS*-, *RR*-, and *meso*-isomers (1:1:2).

although both have the same palmitoyl moiety. The location and stereochemistry of the substituent in the podand significantly influenced the transport behavior. Podands *meso-2* generally offered higher transport rates than the *SS-2* isomers. Since the latter extracted Ag⁺ much more effectively than the former, the release of the complexed Ag⁺ into the aqueous receiving phase is an important process in determining the overall transport rate. Figure 3 shows the relationship between the extraction percentage (Table 2) and the transport rate for all ligands. This plot shows an inverse relationship between the transport rate and extraction percentage.

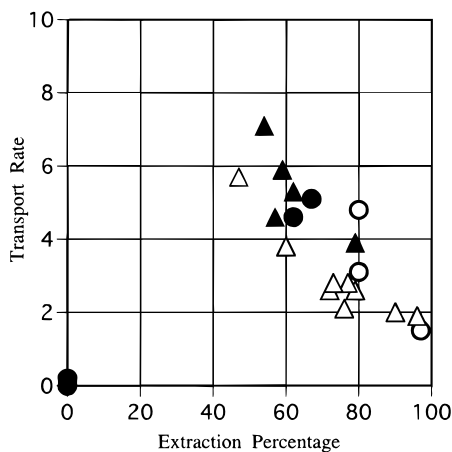


Figure 3. Plot of transport rate vs extraction percentage: ○, podand 1; △, podand 2; ▲, podand 3; ●, podands 4–8.

As reported before,¹⁵ podands which moderately bind the guest Ag^+ effectively transport it.

Thus, we have presented an interesting series of podands capable of specific extraction and transport of Ag^+ . Although several macrocycles have been developed as Ag^+ -specific ligands,¹⁶ the present type of podands have a unique sequence of three pyridine rings which is suitable for Ag^+ binding. Furthermore, stereocontrolled substitution significantly enhances the Ag^+ -binding ability of the pyridine podand. The stereoisomers can, in principle, be considered different ligands of metal cations, but only a few papers have described the effects of stereochemistry of the ligand on metal cation binding.¹⁴ Still et al. prepared certain stereoisomers of the biological ionophore lasalocid with 10 asymmetric substituents in the podand skeleton.³ They demonstrated that the isomer with the natural configuration formed a more stable complex with Na^+ than the other stereoisomers. Our podands have only two chiral substituents, but the effect of stereochemically controlled substitution on the cation-binding properties was clearly observed. Thus, guest-targeted ligand geometry and stereochemically controlled substitution provide a new possibility for the development of specific podand-type ligands, not only for chiral guests but also for achiral metal cations.

Experimental Section

Synthesis of Pyridine Podands. Coupling of Pyridine Alcohol and Acid Chloride (Scheme 4). To an ice-cooled, stirred solution of pyridine alcohol (1 mmol) and DMAP (244 mg, 2 mmol) or Et_3N (0.28 mL, 2 mmol) in anhydrous CH_2Cl_2 (5–30 mL) was dropped a solution of **9a** (102 mg, 0.5 mmol) in anhydrous CH_2Cl_2 (1 mL) during a 3-min period. After

stirring for 10 min at the same temperature and for an additional 30 min at room temperature, the reaction mixture was diluted with CH_2Cl_2 (35–300 mL). The solution was evaporated in *vacuo*, and the residue was purified by column chromatography on silica gel. The following solvent systems were used as eluents: **1a**, $\text{EtOAc}-\text{CH}_2\text{Cl}_2$ (4:1); **1b**, $\text{EtOAc}-\text{CH}_2\text{Cl}_2$ (1:4); **1c**, $\text{EtOAc}-\text{CH}_2\text{Cl}_2$ (1:4); **1e**, $\text{EtOAc}-\text{CH}_2\text{Cl}_2$ (3:7); **1f**, $\text{EtOAc}-\text{hexane}$ (2:3); **SS-2a**, $\text{EtOAc}-\text{hexane}$ (4:1); **SS-2b**, $\text{EtOAc}-\text{hexane}$ (1:4); **SS-2c**, $\text{EtOAc}-\text{hexane}$ (3:7); **SS-3a**, $\text{EtOAc}-\text{hexane}$ (4:1); **SS-3b**, $\text{EtOAc}-\text{hexane}$ (3:7); **SS-3c**, $\text{EtOAc}-\text{hexane}$ (3:7). Due to the poor solubility of **1d**, the reaction mixture was diluted with a large volume of CH_2Cl_2 (ca. 1000 mL) and then refluxed for 1 h. After cooling, the precipitate was collected and recrystallized from CH_2Cl_2 . For the synthesis of **4a, b, 9b** was used instead of **9a**. As eluents, $\text{EtOAc}-\text{hexane}$ (7:3) and $\text{EtOAc}-\text{hexane}$ (1:4) were used in the purification of **4a, b**, respectively.

1a: colorless crystals; mp 171–172 °C (EtOAc); $R_f = 0.50$ ($\text{MeOH}-\text{EtOAc}$, 1:9); IR (KBr) 1740 cm^{-1} ; $^1\text{H NMR}$ (400 MHz, CDCl_3) δ 8.61 (2H, dm, $J = 5.1$ Hz), 8.36 (2H, d, $J = 7.7$ Hz), 8.04 (1H, t, $J = 7.7$ Hz), 7.70 (2H, td, $J = 7.7$ and 1.8 Hz), 7.53 (2H, d, $J = 7.7$ Hz), 7.25 (2H, dd, $J = 5.1$ and 1.8 Hz), 5.58 (4H, s); $^{13}\text{C NMR}$ (100 MHz, CDCl_3) δ 164.1, 155.4, 149.4, 148.2, 138.3, 136.8, 128.3, 122.9, 121.8, 68.0; HRMS (FAB) calcd for $\text{C}_{19}\text{H}_{16}\text{N}_3\text{O}_4$; MH^+ , 350.1141, found m/z 350.1160. Anal. Calcd for $\text{C}_{19}\text{H}_{15}\text{N}_3\text{O}_4$: C, 65.32; H, 4.33; N, 12.03. Found: C, 65.55; H, 4.35; N, 11.78.

1b: colorless crystals; mp 151–152 °C (hexane); $R_f = 0.29$ ($\text{EtOAc}-\text{CH}_2\text{Cl}_2$, 1:9); IR (KBr) 1745 cm^{-1} ; $^1\text{H NMR}$ (400 MHz, CDCl_3) δ 8.34 (2H, d, $J = 7.7$ Hz), 8.02 (1H, t, $J = 7.7$ Hz), 7.70 (2H, t, $J = 7.7$ Hz), 7.47 (2H, d, $J = 7.7$ Hz), 7.38 (2H, d, $J = 7.7$ Hz), 5.53 (4H, s), 4.84 (4H, s), 0.96 (18H, s), 0.12 (12H, s); $^{13}\text{C NMR}$ (100 MHz, CDCl_3) δ 164.2, 161.3, 154.2, 148.3, 138.3, 137.5, 128.2, 119.8, 119.2, 68.1, 65.9, 25.9, 18.3, –5.4; MS (FAB) m/z 638 (MH^+). Anal. Calcd for $\text{C}_{33}\text{H}_{47}\text{N}_3\text{O}_6\text{Si}_2$: C, 62.13; H, 7.43; N, 6.59. Found: C, 61.93; H, 7.54; N, 6.64.

1c: colorless crystals; mp 138–139 °C (EtOAc); $R_f = 0.20$ ($\text{EtOAc}-\text{CH}_2\text{Cl}_2$, 1:9); IR (KBr) 1745, 1735 cm^{-1} ; $^1\text{H NMR}$ (400 MHz, CDCl_3) δ 8.37 (2H, d, $J = 7.9$ Hz), 8.05 (1H, t, $J = 7.9$ Hz), 7.71 (2H, t, $J = 7.7$ Hz), 7.47 (2H, d, $J = 7.7$ Hz), 7.30 (2H, d, $J = 7.7$ Hz), 5.58 (4H, s), 5.23 (4H, s), 2.42 (4H, t, $J = 7.6$ Hz), 1.73–1.63 (4H, m), 1.40–1.18 (48H, m), 0.88 (6H, t, $J = 6.8$ Hz); $^{13}\text{C NMR}$ (75 MHz, CDCl_3) δ 173.4, 164.1, 155.8, 155.1, 148.1, 138.4, 137.6, 128.3, 120.8, 120.7, 67.9, 66.4, 34.2, 31.9, 29.7, 29.6, 29.5, 29.4, 29.3, 29.1, 24.9, 22.7, 14.1; MS (FAB) m/z 887 (MH^+). Anal. Calcd for $\text{C}_{53}\text{H}_{79}\text{N}_3\text{O}_8$: C, 71.83; H, 8.98; N, 4.74. Found: C, 71.87; H, 9.18; N, 4.60.

1d: colorless crystals; mp 248–249 °C (CH_2Cl_2); $R_f = 0.20$ ($\text{MeOH}-\text{EtOAc}$, 2:3); IR (KBr) 1745 cm^{-1} ; $^1\text{H NMR}$ (300 MHz, CDCl_3) δ 8.37 (2H, d, $J = 7.7$ Hz), 8.06 (1H, t, $J = 7.7$ Hz), 7.57 (2H, t, $J = 7.7$ Hz), 7.51 (2H, d, $J = 7.7$ Hz), 7.45 (2H, d, $J = 7.7$ Hz), 5.54 (4H, s); MS (FAB) m/z 510, 508, 506 (MH^+). Anal. Calcd for $\text{C}_{19}\text{H}_{13}\text{Br}_2\text{N}_3\text{O}_4$: C, 45.00; H, 2.58; N, 8.29. Found: C, 45.07; H, 2.86; N, 8.05.

1e: colorless crystals; mp 157–158 °C (hexane); $R_f = 0.40$ ($\text{EtOAc}-\text{CH}_2\text{Cl}_2$, 3:7); IR (KBr) 1750 cm^{-1} ; $^1\text{H NMR}$ (400 MHz, CDCl_3) δ 8.34 (2H, d, $J = 7.8$ Hz), 8.02 (1H, t, $J = 7.8$ Hz), 7.70 (2H, t, $J = 7.8$ Hz), 7.46 (2H, d, $J = 7.8$ Hz), 7.42 (2H, d, $J = 7.8$ Hz), 7.40–7.28 (10H, m), 5.55 (4H, s), 4.69 (4H, s), 4.66 (4H, s); $^{13}\text{C NMR}$ (100 MHz, CDCl_3) δ 164.2, 158.5, 154.7, 148.3, 138.3, 137.9, 137.4, 128.4, 128.2, 127.8, 127.8, 120.6, 120.3, 73.0, 72.9, 68.1; MS (FAB) m/z 590 (MH^+). Anal. Calcd for $\text{C}_{35}\text{H}_{31}\text{N}_3\text{O}_6$: C, 71.29; H, 5.30; N, 7.13. Found: C, 71.39; H, 5.42; N, 6.85.

1f: syrup; $R_f = 0.26$ ($\text{EtOAc}-\text{hexane}$, 2:3); IR (KBr) 1730 cm^{-1} ; $^1\text{H NMR}$ (300 MHz, CDCl_3) δ 8.31 (2H, d, $J = 7.8$ Hz), 7.98 (1H, t, $J = 7.8$ Hz), 7.78 (2H, d, $J = 7.8$ Hz), 7.76 (2H, t, $J = 7.8$ Hz), 7.55–7.47 (12H, m), 7.40 (2H, d, $J = 7.8$ Hz), 7.35–7.19 (18H, m), 5.48 (4H, s), 4.37 (4H, s); $^{13}\text{C NMR}$ (75 MHz, CDCl_3) δ 164.1, 159.2, 154.2, 148.1, 143.7, 138.3, 137.5, 128.6, 128.2, 127.9, 127.1, 120.0, 119.9, 77.2, 68.0, 66.6; HRMS (FAB) calcd for $\text{C}_{59}\text{H}_{48}\text{N}_3\text{O}_6$; MH^+ , 894.3543, found m/z 894.3514.

SS-2a: colorless crystals; mp 78–79 °C (hexane); $R_f = 0.45$ ($\text{EtOAc}-\text{hexane}$, 7:3); $[\alpha]_D^{26} +54.7$ (c 1.59, CHCl_3); IR (KBr) 1740 cm^{-1} ; $^1\text{H NMR}$ (300 MHz, CDCl_3) δ 8.61 (2H, dm, $J =$

(15) (a) Lamb, J. D.; Christensen, J. J.; Oscarson, J. L.; Nielson, B. L.; Asay, B. W.; Izatt, R. M. *J. Am. Chem. Soc.* **1980**, *102*, 6820–6824. (b) Behr, J. P.; Kirch, M.; Lehn, J. M. *J. Am. Chem. Soc.* **1985**, *107*, 241–246.

(16) (a) Lamb, J. D.; Christensen, J. J.; Oscarson, J. L.; Nielson, B. L.; Asay, B. W.; Izatt, R. M. *J. Am. Chem. Soc.* **1980**, *102*, 6820–6824. (b) Behr, J. P.; Kirch, M.; Lehn, J. M. *J. Am. Chem. Soc.* **1985**, *107*, 241–246. (c) Oue, M.; Akama, K.; Kimura, K.; Tanaka, M.; Shono, T. *J. Chem. Soc., Perkin Trans. 1* **1989**, 1675–1678. (d) Craig, A. S.; Katakay, R.; Parker, D.; Adams, H.; Bailey, N.; Schneider, H. *J. Chem. Soc., Chem. Commun.* **1989**, 1870–1872. (e) Tsukube, H.; Minatogawa, M.; Munakata, M.; Toda, M.; Matsumoto, K. *J. Org. Chem.* **1992**, *57*, 542–547. (f) Nabeshima, T.; Tsukada, N.; Nishijima, K.; Ohshiro, H.; Yano, Y. *J. Org. Chem.* **1996**, *61*, 4342–4350. (g) Kumar, S.; Hundal, G.; Kaur, N.; Hundal, M. S.; Singh, H. *Tetrahedron Lett.* **1997**, *38*, 131–132. (h) Vogtle, F.; Ibach, S.; Nieger, M.; Chartroux, C.; Kruger, T.; Stephan, H.; Gloe, K. *J. Chem. Soc., Chem. Commun.* **1997**, 1809–1810.

5.0 Hz), 8.32 (2H, d, $J = 7.8$ Hz), 8.00 (1H, t, $J = 7.8$ Hz), 7.70 (2H, td, $J = 7.8$ and 1.2 Hz), 7.60 (2H, d, $J = 7.8$ Hz), 7.22 (2H, ddd, $J = 7.8$, 5.0, and 1.2 Hz), 6.23 (2H, q, $J = 6.6$ Hz), 1.80 (6H, d, $J = 6.6$ Hz); ¹³C NMR (100 MHz, CDCl₃) δ 163.7, 160.0, 149.2, 148.5, 138.1, 136.8, 127.9, 122.7, 120.5, 74.9, 20.8; MS (EI) m/z (rel intensity) 377 (M⁺, 48), 228 (60), 210 (41), 106 (base). Anal. Calcd for C₂₁H₁₉N₃O₄: C, 66.83; H, 5.07; N, 11.13. Found: C, 66.99; H, 5.18; N, 10.84.

SS-2b: colorless crystals; mp 86–87 °C (hexane); $R_f = 0.30$ (EtOAc–hexane, 1:4); $[\alpha]_D^{25} +39.4$ (c 1.49, CHCl₃); IR (KBr) 1740 cm⁻¹; ¹H NMR (400 MHz, CDCl₃) δ 8.29 (2H, d, $J = 7.7$ Hz), 7.99 (1H, t, $J = 7.7$ Hz), 7.69 (2H, t, $J = 7.7$ Hz), 7.44 (2H, d, $J = 7.7$ Hz), 7.43 (2H, d, $J = 7.7$ Hz), 6.17 (2H, q, $J = 6.6$ Hz), 4.83 (4H, s), 1.76 (6H, d, $J = 6.6$ Hz), 0.94 (18H, s), 0.11 (12H, s); ¹³C NMR (100 MHz, CDCl₃) δ 163.7, 161.0, 158.9, 148.5, 138.1, 137.4, 127.9, 119.0, 118.2, 75.0, 66.0, 25.9, 21.0, 18.3, -5.4; MS (FAB) m/z 666 (MH⁺). Anal. Calcd for C₃₅H₅₁N₃O₆Si₂: C, 63.12; H, 7.72; N, 6.31. Found: C, 62.92; H, 7.71; N, 6.27.

SS-2c: colorless crystals; mp 61–62 °C (hexane); $R_f = 0.55$ (EtOAc–hexane, 2:3); $[\alpha]_D^{25} +14.3$ (c 1.96, CHCl₃); IR (KBr) 1740 cm⁻¹; ¹H NMR (400 MHz, CDCl₃) δ 8.32 (2H, d, $J = 7.8$ Hz), 8.02 (1H, t, $J = 7.8$ Hz), 7.70 (2H, t, $J = 7.8$ Hz), 7.52 (2H, d, $J = 7.8$ Hz), 7.26 (2H, d, $J = 7.8$ Hz), 6.24 (2H, q, $J = 6.7$ Hz), 5.24 (4H, s), 2.42 (4H, t, $J = 7.6$ Hz), 1.78 (6H, d, $J = 6.7$ Hz), 1.67–1.65 (4H, m), 1.32–1.18 (48H, m), 0.88 (6H, t, $J = 7.0$ Hz); ¹³C NMR (100 MHz, CDCl₃) δ 173.2, 163.7, 159.8, 155.6, 148.5, 138.0, 137.4, 127.8, 120.3, 119.1, 74.8, 66.4, 34.1, 31.8, 29.6, 29.5, 29.5, 29.4, 29.2, 29.2, 29.1, 24.9, 22.6, 20.8, 14.0; MS (FAB) m/z 915 (MH⁺). Anal. Calcd for C₅₅H₈₃N₃O₈: C, 72.25; H, 9.15; N, 4.60. Found: C, 72.12; H, 9.33; N, 4.65.

SS-3a: colorless crystals; mp 138–139 °C (hexane); $R_f = 0.53$ (EtOAc–hexane, 4:1); $[\alpha]_D^{25} -80.2$ (c 1.02, CHCl₃); IR (KBr) 1740 cm⁻¹; ¹H NMR (300 MHz, CDCl₃) δ 8.36 (2H, d, $J = 7.8$ Hz), 8.05 (1H, t, $J = 7.8$ Hz), 7.68 (2H, t, $J = 7.8$ Hz), 7.43 (2H, d, $J = 7.8$ Hz), 7.28 (2H, d, $J = 7.8$ Hz), 5.91 (2H, q, $J = 6.7$ Hz), 5.58 (4H, s), 2.13 (6H, s), 1.58 (6H, d, $J = 6.7$ Hz); ¹³C NMR (100 MHz, CDCl₃) δ 170.2, 164.1, 160.1, 155.0, 148.3, 138.3, 137.5, 128.2, 120.4, 119.3, 72.9, 67.9, 21.2, 20.7; MS (FAB) m/z 522 (MH⁺). Anal. Calcd for C₂₇H₂₇N₃O₈: C, 62.18; H, 5.22; N, 8.06. Found: C, 62.30; H, 5.30; N, 7.98.

SS-3b: colorless crystals; mp 137–138 °C (hexane); $R_f = 0.40$ (EtOAc–hexane, 3:7); $[\alpha]_D^{25} -43.4$ (c 1.42, CHCl₃); IR (KBr) 1740 cm⁻¹; ¹H NMR (400 MHz, CDCl₃) δ 8.34 (2H, d, $J = 7.7$ Hz), 8.02 (1H, t, $J = 7.7$ Hz), 7.67 (2H, t, $J = 7.7$ Hz), 7.48 (2H, d, $J = 7.7$ Hz), 7.36 (2H, d, $J = 7.7$ Hz), 5.54 (4H, s), 4.94 (2H, q, $J = 6.6$ Hz), 1.44 (6H, d, $J = 6.6$ Hz), 0.91 (18H, s), 0.07 (6H, s), 0.01 (6H, s); ¹³C NMR (100 MHz, CDCl₃) δ 165.7, 164.2, 153.9, 148.3, 138.3, 137.4, 128.1, 119.6, 118.5, 72.0, 68.1, 25.8, 25.6, 18.2, -4.8, -5.0; MS (EI) m/z (rel intensity) 608 (M⁺ - 57, base), 373 (34), 313 (6), 275 (19). Anal. Calcd for C₃₅H₅₁N₃O₆Si₂: C, 63.12; H, 7.72; N, 6.31. Found: C, 62.86; H, 7.79; N, 6.41.

SS-3c: colorless crystals; mp 118–119 °C (CH₂Cl₂–hexane, 1:19); $R_f = 0.45$ (EtOAc–hexane, 2:3); $[\alpha]_D^{25} -35.7$ (c 1.25, CHCl₃); IR (KBr) 1740, 1730 cm⁻¹; ¹H NMR (400 MHz, CDCl₃) δ 8.36 (2H, d, $J = 7.8$ Hz), 8.05 (1H, t, $J = 7.8$ Hz), 7.68 (2H, t, $J = 7.8$ Hz), 7.43 (2H, d, $J = 7.8$ Hz), 7.28 (2H, d, $J = 7.8$ Hz), 5.92 (2H, q, $J = 6.6$ Hz), 5.57 (4H, s), 2.38 (4H, t, $J = 6.8$ Hz), 1.70–1.60 (4H, m), 1.58 (6H, d, $J = 6.6$ Hz), 1.38–1.20 (48H, m), 0.88 (6H, t, $J = 7.0$ Hz); ¹³C NMR (100 MHz, CDCl₃) δ 172.9, 164.1, 160.4, 155.0, 148.3, 138.2, 137.4, 128.2, 120.3, 119.2, 72.7, 68.0, 34.5, 31.9, 29.6, 29.6, 29.6, 29.4, 29.3, 29.2, 29.1, 24.9, 22.6, 20.8, 14.1; MS (FAB) m/z 915 (MH⁺). Anal. Calcd for C₅₅H₈₃N₃O₈: C, 72.25; H, 9.15; N, 4.60. Found: C, 72.15; H, 9.44; N, 4.76.

4a: colorless crystals; mp 69–70 °C (hexane); $R_f = 0.49$ (EtOAc); IR (KBr) 1720 cm⁻¹; ¹H NMR (400 MHz, CDCl₃) δ 8.81 (1H, t, $J = 1.8$ Hz), 8.60 (2H, ddd, $J = 4.8$, 1.8, and 0.7 Hz), 8.30 (2H, dd, $J = 7.7$ and 1.8 Hz), 7.70 (2H, td, $J = 7.7$ and 1.8 Hz), 7.55 (1H, t, $J = 7.7$ Hz), 7.43 (2H, d, $J = 7.7$ Hz), 7.23 (2H, ddd, $J = 7.7$, 4.8, and 0.7 Hz), 5.49 (4H, s); ¹³C NMR (100 MHz, CDCl₃) δ 165.3, 155.6, 149.5, 136.8, 134.2, 131.0, 130.3, 128.7, 122.9, 121.8, 67.5; MS (EI) m/z (rel intensity) 348 (MH⁺, 5), 347 (base), 240 (25), 213 (50). Anal. Calcd for

C₂₀H₁₆N₂O₄: C, 68.96; H, 4.63; N, 8.04. Found: C, 69.22; H, 4.75; N, 7.75.

SS-4b: colorless crystals; mp 82–83 °C (EtOAc); $R_f = 0.53$ (EtOAc–hexane, 1:4); $[\alpha]_D^{25} -37.3$ (c 1.94, CHCl₃); IR (KBr) 1730 cm⁻¹; ¹H NMR (400 MHz, CDCl₃) δ 8.84 (1H, t, $J = 1.6$ Hz), 8.33 (2H, dd, $J = 7.8$ and 1.6 Hz), 7.71 (2H, t, $J = 7.8$ Hz), 7.58 (1H, t, $J = 7.8$ Hz), 7.34 (2H, d, $J = 7.8$ Hz), 7.28 (2H, d, $J = 7.8$ Hz), 5.92 (2H, q, $J = 6.7$ Hz), 5.51 (4H, s), 2.38 (4H, t, $J = 7.5$ Hz), 1.68–1.61 (4H, m), 1.56 (6H, d, $J = 6.7$ Hz), 1.39–1.20 (48H, m), 0.88 (6H, t, $J = 7.3$ Hz); ¹³C NMR (100 MHz, CDCl₃) δ 172.9, 165.2, 160.5, 155.2, 137.4, 134.2, 131.0, 130.5, 128.7, 120.2, 119.2, 72.7, 67.4, 34.5, 31.9, 29.6, 29.6, 29.6, 29.4, 29.3, 29.2, 29.1, 24.9, 22.6, 20.8, 14.1; MS (FAB) m/z 914 (MH⁺). Anal. Calcd for C₅₆H₈₄N₂O₈: C, 73.65; H, 9.27; N, 3.07. Found: C, 73.65; H, 9.52; N, 3.03.

Preparation of 5. To a mixture of 2,6-pyridinedimethanol (300 mg, 2.16 mmol) and ethyl picolinate (0.874 mL, 6.47 mmol) in toluene (25 mL) was added anhydrous K₂CO₃ (50 mg). After refluxing for 1 h and cooling, dry ether (80 mL) was added and the mixture was filtered. The filtrate was evaporated *in vacuo*, and the residue was chromatographed on silica gel with EtOAc as eluent to give **5** (527 mg) in 70% yield: colorless crystals; mp 138–140 °C (ether); $R_f = 0.37$ (MeOH–EtOAc, 1:9); IR (KBr) 1740 cm⁻¹; ¹H NMR (300 MHz, CDCl₃) δ 8.80 (2H, dm, $J = 7.8$ Hz), 8.20 (2H, d, $J = 7.8$ Hz), 7.88 (2H, td, $J = 7.8$ and 1.8 Hz), 7.74 (2H, d, $J = 7.8$ Hz), 7.52 (2H, ddd, $J = 7.8$, 4.8, and 1.2 Hz), 7.43 (2H, d, $J = 7.8$ Hz), 5.59 (4H, s); ¹³C NMR (100 MHz, CDCl₃) δ 164.7, 155.3, 149.9, 147.6, 137.6, 137.0, 127.1, 125.4, 120.8, 67.6; MS (FAB) m/z 350 (MH⁺). Anal. Calcd for C₅₅H₈₃N₃O₈: C, 65.32; H, 4.33; N, 12.03. Found: C, 65.29; H, 4.33; N, 11.92.

Synthesis of meso-Podands (Scheme 5). Preparation of 30. To a mixture of **9a** (299 mg, 1.47 mmol) and Et₃N (410 μL, 2.94 mmol) in anhydrous CH₂Cl₂ (10 mL) was added a solution of **S-17** (297 mg, 1.47 mmol) in anhydrous CH₂Cl₂ (3.5 mL) at -78 °C under Ar atmosphere. The mixture was warmed slowly to -15 °C during 30 min, and then a solution of **R-16** (181 mg, 1.47 mmol) in CH₂Cl₂ (3.5 mL) was added. The mixture was stirred for 10 min at the same temperature, then diluted with CH₂Cl₂ (180 mL), and worked up. The residual oil was purified by chromatography on silica gel with EtOAc–hexane (3:2) as eluent to give **30** (428 mg) in 64% yield along with symmetrical coupling product (73 mg) in 9% yield.

30: colorless crystals; mp 56–57 °C (hexane); $R_f = 0.45$ (EtOAc–hexane, 7:3); $[\alpha]_D^{25} +11.7$ (c 1.99, CHCl₃); IR (KBr) 1735 cm⁻¹; ¹H NMR (300 MHz, CDCl₃) δ 8.61 (1H, dm, $J = 4.8$ Hz), 8.34 (1H, d, $J = 7.7$ Hz), 8.33 (1H, d, $J = 7.7$ Hz), 8.04 (1H, t, $J = 7.7$ Hz), 7.70 (1H, td, $J = 7.7$ and 1.7 Hz), 7.60 (1H, d, $J = 7.7$ Hz), 7.58 (1H, d, $J = 7.7$ Hz), 7.55 (1H, t, $J = 7.7$ Hz), 7.41 (1H, d, $J = 7.7$ Hz), 7.23 (1H, ddm, $J = 7.7$ and 4.9 Hz), 6.23 (1H, q, $J = 6.7$ Hz), 6.18 (1H, q, $J = 6.7$ Hz), 1.81 (3H, d, $J = 6.7$ Hz), 1.79 (3H, d, $J = 6.7$ Hz); ¹³C NMR (75 MHz, CDCl₃) δ 163.6, 163.6, 161.5, 159.8, 149.2, 148.4, 148.2, 141.4, 139.2, 138.2, 136.9, 128.1, 128.0, 127.1, 122.8, 120.5, 119.1, 74.8, 74.1, 20.8, 20.8; HRMS (EI) calcd for C₂₁H₁₈BrN₃O₄, M⁺, 455.0481 and 457.0460, found m/z 455.0456 and 457.0431.

Preparation of meso-2a. To a degassed anhydrous benzene solution (2.5 mL) of **30** (201 mg, 0.44 mmol) and Bu₃SnH (142 μL, 0.53 mmol) was added triethylborane (88 μL of 1.0 M hexane solution) at room temperature. The mixture was stirred for 2 h at room temperature, and then the reaction was quenched with saturated aqueous NaHCO₃ (1 mL). The mixture was diluted with CH₂Cl₂ (40 mL) and worked up. The residue was chromatographed on silica gel with EtOAc–hexane (7:3) as eluent to give **meso-2a** (100 mg) in 60% yield: colorless crystals; mp 98–99 °C (hexane). R_f value, ¹H NMR, ¹³C NMR, IR, and MS spectral data were exactly the same as those of **SS-2a**.

Preparation of 31. To a mixture of **9a** (676 mg, 3.31 mmol) and Et₃N (1.38 mL, 9.94 mmol) in anhydrous CH₂Cl₂ (30 mL) was added a solution of **S-18** (886 mg, 3.31 mmol) in anhydrous CH₂Cl₂ (10 mL) at -78 °C under Ar atmosphere. The mixture was warmed slowly to -15 °C during 30 min, and then a solution of **R-20** (1.31 g, 3.31 mmol) in CH₂Cl₂ (10 mL) was

added. The mixture was stirred for 10 min at the same temperature, then allowed to warm to room temperature, and stirred for 7 h. The reaction mixture was diluted with CH_2Cl_2 (100 mL) and worked up. The crude product was purified by column chromatography on silica gel with EtOAc–hexane (3:2) as eluent followed by HPLC purification (silica gel, EtOAc–hexane (7:13)) to give **31** (943 mg) in 36% yield along with **SS-2b** (243 mg) in 11% yield. **31**: colorless oil; $R_f = 0.38$ (EtOAc–hexane, 3:7); $[\alpha]_D^{26} -0.44$ (c 1.47, CHCl_3); IR (neat) 1750 and 1730 cm^{-1} ; $^1\text{H NMR}$ (400 MHz, CDCl_3) δ 8.29 (1H, dd, $J = 7.8$ and 1.1 Hz), 8.28 (1H, dd, $J = 7.8$ and 1.1 Hz), 7.97 (1H, t, $J = 7.8$ Hz), 7.73 (1H, t, $J = 7.8$ Hz), 7.70 (1H, dm, $J = 7.8$ Hz), 7.68 (1H, t, $J = 7.8$ Hz), 7.53–7.49 (6H, m), 7.47 (1H, d, $J = 7.8$ Hz), 7.44 (1H, d, $J = 7.8$ Hz), 7.43 (1H, d, $J = 7.8$ Hz), 7.34–7.21 (9H, m), 6.18 (1H, q, $J = 6.7$ Hz), 6.14 (1H, q, $J = 6.7$ Hz), 4.84 (2H, s), 4.29 (1H, s), 4.28 (1H, s), 1.77 (3H, d, $J = 6.7$ Hz), 1.72 (3H, d, $J = 6.7$ Hz), 0.96 (9H, s), 0.12 (6H, s); $^{13}\text{C NMR}$ (75 MHz, CDCl_3) δ 163.7, 163.7, 160.9, 159.2, 159.0, 158.9, 148.4, 143.7, 138.1, 137.5, 128.6, 127.9, 127.9, 127.1, 119.6, 118.9, 118.3, 118.1, 87.1, 75.0, 66.7, 65.9, 25.9, 21.1, 21.0, 18.3, –5.4; HRMS (FAB) calcd for $\text{C}_{48}\text{H}_{52}\text{N}_3\text{O}_6\text{Si}$, MH^+ , 794.3626, found m/z 794.3641.

Preparation of 32. A mixture of **31** (385 mg, 1.1 mmol) and ZnBr_2 (1.09 g, 4.85 mmol) in CH_2Cl_2 (8 mL) was stirred for 10 min at room temperature. The mixture was diluted with CH_2Cl_2 (90 mL) and worked up. The crude product was purified by column chromatography on silica gel with EtOAc–hexane (3:2) as eluent to give **32** (231 mg) in 88% yield: syrup; $R_f = 0.33$ (EtOAc–hexane, 7:3); $[\alpha]_D^{26} -1.28$ (c 1.93, CHCl_3); IR (KBr) 3300, 1740 cm^{-1} ; $^1\text{H NMR}$ (300 MHz, CDCl_3) δ 8.32 (1H, d, $J = 7.8$ Hz), 8.32 (1H, d, $J = 7.8$ Hz), 8.01 (1H, t, $J = 7.8$ Hz), 7.69 (1H, t, $J = 7.8$ Hz), 7.67 (1H, t, $J = 7.8$ Hz), 7.47 (1H, d, $J = 7.8$ Hz), 7.44 (1H, d, $J = 7.8$ Hz), 7.41 (1H, d, $J = 7.8$ Hz), 7.15 (1H, d, $J = 7.8$ Hz), 6.23 (1H, q, $J = 6.7$ Hz), 6.17 (1H, q, $J = 6.7$ Hz), 4.84 (2H, s), 4.75 (2H, d, $J = 4.8$ Hz), 4.16 (1H, t, $J = 4.8$ Hz), 1.80 (3H, d, $J = 6.7$ Hz), 1.77 (3H, d, $J = 6.7$ Hz), 0.95 (9H, s), 0.11 (6H, s); $^{13}\text{C NMR}$ (75 MHz, CDCl_3) δ 163.8, 163.7, 161.1, 158.8, 158.7, 158.6, 148.4, 148.4, 138.2, 137.6, 137.5, 128.1, 128.1, 119.6, 119.1, 119.1, 118.3, 75.1, 74.6, 65.9, 63.8, 25.9, 21.0, 20.8, 18.3, –5.4; HRMS (FAB) calcd for $\text{C}_{29}\text{H}_{38}\text{N}_3\text{O}_6\text{Si}$, MH^+ , 552.2530, found m/z 552.2514.

Preparation of meso-2b. $t\text{-BuMe}_2\text{SiCl}$ (97 mg, 0.64 mmol) was added to a mixture of **32** (231 mg, 0.43 mmol) and DMAP (105 mg, 0.86 mmol) in CH_2Cl_2 (3 mL) at room temperature. After being stirred for 30 min, the reaction mixture was diluted with CH_2Cl_2 (100 mL) and worked up. The crude product was purified by silica gel chromatography with EtOAc–hexane (3:2) as eluent to give **meso-2b** (265 mg) in 93% yield: colorless crystals, mp 99–100 °C (hexane). The R_f value, $^1\text{H NMR}$, $^{13}\text{C NMR}$, IR, and MS spectral data were exactly the same as those of **SS-2b**.

Preparation of 33. To a mixture of **9a** (195 mg, 0.95 mmol) and Et_3N (400 μL , 2.86 mmol) in anhydrous CH_2Cl_2 (6 mL) was added a solution of **S-18** (255 mg, 0.95 mmol) in anhydrous CH_2Cl_2 (2 mL) at –78 °C under Ar atmosphere. The mixture was warmed slowly to –15 °C during 30 min, and then a solution of **R-19** (299 mg, 0.763 mmol) in CH_2Cl_2 (2 mL) was added. After stirring for 1 h at the same temperature and for 1 h at room temperature, the reaction mixture was diluted with CH_2Cl_2 (50 mL) and worked up. The crude product was purified by column chromatography on silica gel with EtOAc–hexane (3:7) as eluent followed by HPLC purification (silica gel, EtOAc–hexane (1:3) as eluent) to give **33** (408 mg) in 68% yield along with **SS-2c** (48 mg) in 8% yield. **33**: colorless oil; $R_f = 0.26$ (EtOAc–hexane, 3:7); $[\alpha]_D^{25} +0.71$ (c 1.39, CHCl_3); IR (neat) 1745, 1730 cm^{-1} ; $^1\text{H NMR}$ (300 MHz, CDCl_3) δ 8.31 (2H, d, $J = 7.7$ Hz), 8.00 (1H, t, $J = 7.7$ Hz), 7.69 (1H, t, $J = 7.7$ Hz), 7.68 (1H, t, $J = 7.7$ Hz), 7.53 (1H, d, $J = 7.7$ Hz), 7.44 (2H, d, $J = 7.7$ Hz), 7.25 (1H, d, $J = 7.7$ Hz), 6.21 (1H, q, $J = 6.7$ Hz), 6.18 (1H, q, $J = 6.7$ Hz), 5.23 (2H, s), 4.84 (2H, s), 2.41 (2H, t, $J = 7.5$ Hz), 1.78 (3H, d, $J = 6.7$ Hz), 1.77 (3H, d, $J = 6.7$ Hz), 1.69–1.64 (2H, m), 1.29–1.16 (24H, m), 0.95 (9H, s), 0.87 (3H, t, $J = 6.8$ Hz), 0.12 (6H, s); $^{13}\text{C NMR}$ (100 MHz, CDCl_3) δ 173.4, 163.8, 161.0, 159.9, 159.0, 155.6, 148.6, 148.5, 138.1, 137.5, 137.5, 128.0, 120.4, 119.2, 119.0, 118.2, 75.1, 74.9,

66.5, 66.0, 34.2, 31.9, 29.7, 29.6, 29.5, 29.4, 29.3, 29.2, 29.2, 25.9, 24.9, 22.7, 21.0, 21.0, 18.3, 14.1, –5.4; HRMS (FAB) calcd for $\text{C}_{45}\text{H}_{68}\text{N}_3\text{O}_7\text{Si}$, MH^+ , 790.4827, found m/z 790.4849.

Preparation of 34. To a THF solution (4 mL) of **33** (365 mg, 0.46 mmol) was added Bu_4NF (0.46 mL of a 1 M THF solution) at room temperature. The mixture was stirred for 40 min, diluted with EtOAc (70 mL), and worked up. The crude product was purified by column chromatography on silica gel with EtOAc–hexane (7:3) as eluent to give **34** (102 mg) in 33% yield. A compound with the palmitoyl group hydrolyzed was formed as a side product. **34**: colorless oil; $R_f = 0.35$ (EtOAc–hexane, 7:3); $[\alpha]_D^{25} -0.46$ (c 2.47, CHCl_3); IR (neat) 3400, 1740, 1720, 1710 cm^{-1} ; $^1\text{H NMR}$ (300 MHz, CDCl_3) δ 8.33 (1H, d, $J = 7.8$ Hz), 8.33 (1H, d, $J = 7.8$ Hz), 8.02 (1H, t, $J = 7.8$ Hz), 7.70 (1H, d, $J = 7.8$ Hz), 7.68 (1H, d, $J = 7.8$ Hz), 7.50 (1H, t, $J = 7.8$ Hz), 7.50 (1H, t, $J = 7.8$ Hz), 7.26 (1H, d, $J = 7.8$ Hz), 7.16 (1H, d, $J = 7.8$ Hz), 6.24 (1H, q, $J = 6.7$ Hz), 6.22 (1H, q, $J = 6.7$ Hz), 5.24 (2H, s), 4.77 (2H, s), 2.42 (2H, t, $J = 6.4$ Hz), 1.81 (3H, d, $J = 6.7$ Hz), 1.79 (3H, d, $J = 6.7$ Hz), 1.72–1.62 (2H, m), 1.38–1.20 (24H, m), 0.88 (3H, t, $J = 7.0$ Hz); $^{13}\text{C NMR}$ (100 MHz, CDCl_3) δ 173.4, 163.8, 163.7, 159.8, 158.8, 158.5, 155.6, 148.5, 148.4, 138.2, 137.5, 128.0, 128.0, 120.4, 119.5, 119.2, 118.9, 74.9, 74.6, 66.4, 63.8, 34.2, 31.9, 29.6, 29.6, 29.5, 29.4, 29.3, 29.2, 29.1, 24.9, 22.6, 20.9, 20.8, 14.1; HRMS (FAB) calcd for $\text{C}_{39}\text{H}_{54}\text{N}_3\text{O}_7$, MH^+ , 676.3962, found m/z 676.3959.

Preparation of meso-2c. Palmitoyl chloride (32 mg, 0.157 mmol) was added to a mixture of **34** (96 mg, 0.143 mmol) and DMAP (88 mg, 0.072 mmol) in anhydrous CH_2Cl_2 (2 mL) at room temperature. The mixture was stirred for 5 min, quenched with water (5 mL), and extracted with EtOAc–hexane (1:1, 30 mL). The crude product was purified by silica gel chromatography with EtOAc–hexane (2:3) as eluent to give **meso-2c** (120 mg) in 91% yield: colorless crystals; mp 54–55 °C (hexane). R_f value, $^1\text{H NMR}$, $^{13}\text{C NMR}$, IR, and MS spectral data were exactly the same as those of **SS-2c**.

Synthesis of Pyridinemethanol Precursors (Scheme 1). **Preparation of 12.** A mixture of 2,6-pyridinedimethanol (765 mg, 5.5 mmol), palmitoyl chloride (1.36 g, 4.95 mmol), and Et_3N (1.15 mL, 8.25 mmol) was stirred in 120 mL of THF– CH_2Cl_2 (1:1) for 1.5 h at room temperature. Then the solvent was removed in *vacuo*, and the residue was dissolved in CH_2Cl_2 (120 mL) and worked up. The crude product was purified by column chromatography on silica gel with EtOAc–hexane (2:3) as eluent to give **12** (1.3 g) in 70% yield along with the dipalmitate (531 mg) in 17% yield. **12**: colorless crystals; mp 69–70 °C (hexane); $R_f = 0.50$ (EtOAc–hexane, 2:3); IR (KBr) 3380, 1735 cm^{-1} ; $^1\text{H NMR}$ (300 MHz, CDCl_3) δ 7.71 (1H, t, $J = 7.7$ Hz), 7.26 (1H, d, $J = 7.7$ Hz), 7.20 (1H, d, $J = 7.7$ Hz), 5.23 (2H, s), 4.76 (2H, s), 3.95 (1H, br s), 2.42 (2H, t, $J = 7.5$ Hz), 1.67 (2H, m), 1.40–1.17 (24H, m), 0.88 (3H, t, $J = 6.7$ Hz); $^{13}\text{C NMR}$ (75 MHz, CDCl_3) δ 173.4, 158.7, 154.9, 137.4, 120.1, 119.6, 66.2, 63.8, 34.2, 31.9, 29.7, 29.6, 29.4, 29.3, 29.2, 29.1, 24.9, 22.7, 14.1; MS (FAB) m/z 378 (MH^+). Anal. Calcd for $\text{C}_{23}\text{H}_{39}\text{NO}_3$: C, 73.17; H, 10.41; N, 3.71. Found: C, 73.30; H, 10.29; N, 3.62.

Preparation of 15. A mixture of 2,6-pyridinedimethanol (100 mg, 0.72 mmol), trityl chloride (1.36 g, 0.72 mmol), and Et_3N (0.3 mL, 2.16 mmol) was stirred in 5.5 mL of THF– CH_2Cl_2 (1:10) for 7 h at room temperature. Then, the solvent was removed in *vacuo*, and the residue was dissolved in EtOAc (100 mL) and worked up. The crude product was purified by column chromatography on silica gel with EtOAc–hexane (3:7) as eluent to give **15** (174 mg) in 64% yield along with the ditrityl product (24 mg) in 5% yield. **15**: colorless crystals; mp 115–116 °C (hexane); $R_f = 0.49$ EtOAc–hexane (1:1); IR (KBr) 3230 cm^{-1} ; $^1\text{H NMR}$ (400 MHz, CDCl_3) δ 7.70 (1H, t, $J = 7.6$ Hz), 7.65 (1H, d, $J = 7.6$ Hz), 7.51 (6H, d, $J = 7.4$ Hz), 7.30 (6H, t, $J = 7.4$ Hz), 7.23 (3H, t, $J = 7.4$ Hz), 7.08 (1H, d, $J = 7.6$ Hz), 4.66 (2H, s), 4.34 (2H, s), 3.78 (1H, br s); $^{13}\text{C NMR}$ (100 MHz, CDCl_3) δ 158.2, 157.9, 143.8, 137.3, 128.6, 127.9, 127.1, 119.3, 118.6, 87.3, 66.8, 63.8; MS (FAB) m/z 382 (MH^+). Anal. Calcd for $\text{C}_{26}\text{H}_{23}\text{NO}_2$: C, 81.86; H, 6.08; N, 3.67. Found: C, 81.97; H, 6.11; N, 3.75.

Preparation of 24. To a DMF (16 mL) suspension of NaH (120 mg, 3 mmol, 60% in mineral oil) was added **15** (956 mg, 2.51 mmol) in 12 mL of DMF–THF (2:1) at 0 °C. The mixture was stirred for 30 min, and benzyl bromide (0.36 mL, 3.01 mmol) was added. The ice bath was removed after 30 min, and stirring was further continued for 12 h. The mixture was diluted with 120 mL of EtOAc–hexane (3:7) and worked up. The crude product was purified by silica gel chromatography with EtOAc–hexane (1:4) as eluent to give **24** (1.09 g) in 93% yield: colorless crystals; mp 115–117 °C (hexane); $R_f = 0.23$ (EtOAc–hexane, 1:9); ¹H NMR (400 MHz, CDCl₃) δ 7.76 (1H, t, $J = 7.7$ Hz), 7.70 (1H, d, $J = 7.7$ Hz), 7.51–7.48 (6H, m), 7.37–7.20 (15H, m), 4.61 (2H, s), 4.59 (2H, s), 4.35 (2H, s); ¹³C NMR (100 MHz, CDCl₃) δ 158.8, 157.5, 143.8, 138.0, 137.3, 128.7, 128.4, 127.9, 127.8, 127.7, 127.1, 119.6, 119.3, 87.3, 73.1, 72.9, 66.9; MS (FAB) m/z 472 (MH⁺). Anal. Calcd for C₃₃H₂₉NO₂: C, 84.05; H, 6.20; N, 2.97. Found: C, 83.85; H, 6.29; N, 3.08.

Preparation of 14. To a stirred solution of **24** (420 mg, 0.89 mmol) in 10 mL of MeOH–CH₂Cl₂ (3:2) was added concentrated HCl (10 mL) at 0 °C. After stirring for 20 min at room temperature, saturated aqueous NaHCO₃ (100 mL) was added, and the solvent was removed in *vacuo*. The residue was dissolved in water (5 mL) and extracted with CH₂Cl₂ (70 mL). The crude product was chromatographed on silica gel with EtOAc–hexane (1:1) as eluent to give **14** (196 mg) in 96% yield: colorless oil; $R_f = 0.30$ (EtOAc–hexane, 3:2); IR (neat) 3380 cm⁻¹; ¹H NMR (400 MHz, CDCl₃) δ 7.67 (1H, t, $J = 7.7$ Hz), 7.42–7.26 (6H, m), 7.14 (1H, d, $J = 7.7$ Hz), 4.72 (2H, s), 4.66 (2H, s), 4.63 (2H, s), 4.15 (1H, br s); ¹³C NMR (100 MHz, CDCl₃) δ 158.5, 157.5, 137.8, 137.3, 128.4, 127.7, 119.8, 119.1, 72.8, 72.7, 64.0; HRMS (FAB) calcd for C₁₄H₁₆NO₂, MH⁺, 230.1181, found m/z 230.1198.

Synthesis of Chiral Pyridineethanol Precursors (Schemes 2 and 3). Preparation of S-25. To an ice-cooled solution of **S-25** (507 mg, 3.31 mmol) and Et₃N (0.69 mL, 4.96 mmol) in CH₂Cl₂ (33 mL) was added acetic anhydride (0.32 mL, 3.4 mmol). The mixture was stirred for 2 h at 0 °C. Ice water (20 mL) was added, and the mixture was extracted with EtOAc (150 mL). The crude product was purified by silica gel column chromatography with EtOAc–hexane (1:1) as eluent. Oily acetate **26** (582 mg) was obtained in 96% yield: colorless oil; $R_f = 0.35$ (EtOAc–hexane, 1:1); $[\alpha]_D^{26} -3.89$ (*c* 1.97, CHCl₃); IR (neat) 3420, 1740 cm⁻¹; ¹H NMR (300 MHz, CDCl₃) δ 7.72 (1H, t, $J = 7.8$ Hz), 7.26 (1H, d, $J = 7.8$ Hz), 7.24 (1H, d, $J = 7.8$ Hz), 5.23 (2H, s), 4.90 (1H, q, $J = 6.6$ Hz), 4.45 (1H, br s), 2.18 (3H, s), 1.50 (3H, d, $J = 6.6$ Hz); ¹³C NMR (75 MHz, CDCl₃) δ 170.6, 162.7, 154.2, 137.5, 119.9, 118.9, 68.5, 66.5, 24.1, 20.9; HRMS (FAB) calcd for C₁₀H₁₄NO₃, MH⁺, 196.0973, found m/z 196.0957.

Preparation of S-27. A mixture of **26** (583 mg, 3.18 mmol), imidazole (650 mg, 9.55 mmol), and *t*-BuMe₂SiCl (528 mg, 3.5 mmol) in DMF (5 mL) was stirred for 1 h at room temperature. The reaction mixture was diluted with 200 mL of EtOAc–hexane (3:7) and worked up. The crude product was purified by silica gel column chromatography with EtOAc–hexane (1:4) as eluent to give **27** (953 mg) in 98% yield: colorless oil; $R_f = 0.25$ (EtOAc–hexane, 1:9); $[\alpha]_D^{27} -38.5$ (*c* 2.62, CHCl₃); IR (neat) 1750 cm⁻¹; ¹H NMR (300 MHz, CDCl₃) δ 7.65 (1H, t, $J = 7.7$ Hz), 7.44 (1H, d, $J = 7.7$ Hz), 7.14 (1H, d, $J = 7.7$ Hz), 5.14 (2H, s), 4.90 (1H, q, $J = 6.6$ Hz), 2.10 (3H, s), 1.40 (3H, d, $J = 6.6$ Hz), 0.87 (9H, s), 0.03 (3H, s), -0.04 (3H, s); ¹³C NMR (75 MHz, CDCl₃) δ 170.5, 165.7, 154.1, 137.2, 119.6, 118.3, 71.8, 66.8, 25.7, 25.5, 20.8, 18.1, -4.9, -5.1; HRMS (FAB) calcd for C₁₆H₂₈NO₃Si, MH⁺, 310.1838, found m/z 310.1841.

Preparation of S-22. To a methanol solution of **27** (681 mg, 2.2 mmol) was added anhydrous K₂CO₃ (608 mg, 4.4 mmol), and the mixture was stirred for 30 min. After the solvent was removed, water (5 mL) was added to the residue and the mixture was extracted with EtOAc (70 mL). The crude product was purified by chromatography on silica gel with EtOAc–hexane (3:7) as eluent to give **22** (566 mg) in 96% yield: colorless oil; $R_f = 0.45$ (EtOAc–hexane, 3:7); $[\alpha]_D^{22} -44.7$ (*c* 1.97, CHCl₃); IR (neat) 3400 cm⁻¹; ¹H NMR (300 MHz, CDCl₃) δ 7.66 (1H, t, $J = 7.7$ Hz), 7.43 (1H, d, $J = 7.7$ Hz),

7.07 (1H, d, $J = 7.7$ Hz), 4.93 (1H, q, $J = 6.5$ Hz), 4.72 (2H, s), 4.12 (1H, br s), 1.44 (3H, d, $J = 6.5$ Hz), 0.91 (9H, s), 0.08 (3H, s), 0.01 (3H, s); ¹³C NMR (75 MHz, CDCl₃) δ 164.7, 157.3, 137.3, 118.3, 117.8, 71.8, 63.7, 25.8, 25.4, 18.2, -4.8, -5.0; HRMS (FAB) calcd for C₁₄H₂₆NO₂Si, MH⁺, 268.1733, found m/z 268.1725.

Preparation of S-19. To an ice-cooled solution of **S-25** (153 mg, 1 mmol) and Et₃N (0.21 mL, 1.5 mmol) in CH₂Cl₂ (10 mL) was dropped palmitoyl chloride (275 mg, 1 mmol) in CH₂Cl₂ (1 mL). The mixture was stirred for 15 min at 0 °C and diluted with EtOAc (70 mL). The crude product was chromatographed on silica gel with EtOAc–hexane (2:3) as eluent to give **19** (368 mg) in 94% yield: colorless crystals; mp 35–36 °C (hexane); $R_f = 0.28$ (EtOAc–hexane, 3:7); $[\alpha]_D^{25} -1.72$ (*c* 2.00, CHCl₃); IR (KBr) 3420, 1740 cm⁻¹; ¹H NMR (400 MHz, CDCl₃) δ 7.70 (1H, t, $J = 7.7$ Hz), 7.24 (1H, d, $J = 7.7$ Hz), 7.20 (1H, d, $J = 7.7$ Hz), 5.23 (2H, s), 4.88 (1H, q, $J = 6.6$ Hz), 3.90 (1H, br s), 2.42 (2H, t, $J = 7.6$ Hz), 1.73–1.62 (2H, m), 1.50 (3H, d, $J = 6.6$ Hz), 1.38–1.18 (24H, m), 0.88 (3H, t, $J = 6.8$ Hz); ¹³C NMR (100 MHz, CDCl₃) δ 173.4, 162.7, 154.6, 137.5, 119.9, 118.8, 68.5, 66.3, 34.2, 31.9, 29.7, 29.6, 29.6, 29.4, 29.3, 29.2, 29.1, 24.9, 24.2, 22.7, 14.1; MS (EI) m/z (rel intensity) 391 (M⁺, base), 376 (22), 348 (9), 279 (22), 256 (35). Anal. Calcd for C₂₄H₄₁NO₃: C, 73.61; H, 10.55; N, 3.58. Found: C, 73.47; H, 10.76; N, 3.61. **R-19** was obtained exactly in the same manner described for **S-18** but starting from **R-25**.

Preparation of S-28. **S-28** was obtained by acetylation of **S-18** in 94% yield. The method was the same as described for **S-26** except EtOAc–hexane (1:9) was employed as eluent for column chromatography: colorless oil; $R_f = 0.55$ (EtOAc–hexane, 1:4); $[\alpha]_D^{26} -61.9$ (*c* 2.02, CHCl₃); IR (neat) 1740 cm⁻¹; ¹H NMR (400 MHz, CDCl₃) δ 7.69 (1H, t, $J = 7.7$ Hz), 7.42 (1H, d, $J = 7.7$ Hz), 7.18 (1H, d, $J = 7.7$ Hz), 5.86 (1H, q, $J = 6.7$ Hz), 4.83 (2H, s), 2.11 (3H, s), 1.56 (3H, d, $J = 6.7$ Hz), 0.95 (9H, s), 0.12 (6H, s); ¹³C NMR (100 MHz, CDCl₃) δ 169.9, 160.9, 159.2, 137.1, 118.7, 118.1, 73.0, 66.0, 25.8, 21.1, 20.7, 18.2, -5.5; HRMS (FAB) calcd for C₁₆H₂₈NO₃Si, MH⁺, 310.1839, found m/z 310.1858.

Preparation of S-21. **S-21** was obtained in 97% yield by desilylation of **S-28** with Bu₄NF. The method was the same as described for **S-25** except using EtOAc–hexane (7:3) as the eluent for column chromatography: colorless oil; $R_f = 0.30$ (EtOAc–hexane (1:1)); $[\alpha]_D^{26} -93.3$ (*c* 1.85, CHCl₃); IR (neat) 3410, 1740 cm⁻¹; ¹H NMR (300 MHz, CDCl₃) δ 7.69 (1H, t, $J = 7.7$ Hz), 7.25 (1H, d, $J = 7.7$ Hz), 7.17 (1H, d, $J = 7.7$ Hz), 5.91 (1H, q, $J = 6.7$ Hz), 4.75 (2H, s), 4.16 (1H, br s), 2.13 (3H, s), 1.59 (3H, d, $J = 6.7$ Hz); ¹³C NMR (75 MHz, CDCl₃) δ 170.2, 159.1, 158.4, 137.4, 119.3, 118.7, 72.8, 63.7, 21.2, 20.6; HRMS (EI) calcd for C₁₀H₁₃NO₃, M⁺, 195.0896, found m/z 195.0911.

Preparation of S-29. **S-29** was obtained in 95% yield by acylation of **S-18** with palmitoyl chloride. The synthetic method was the same as described for **S-19** except using EtOAc–hexane (1:19) as the eluent for column chromatography: colorless oil; $R_f = 0.47$ (EtOAc–hexane, 1:9); $[\alpha]_D^{25} -34.9$ (*c* 1.05, CHCl₃); IR (neat) 1740 cm⁻¹; ¹H NMR (400 MHz, CDCl₃) δ 7.67 (1H, t, $J = 7.7$ Hz), 7.40 (1H, d, $J = 7.7$ Hz), 7.16 (1H, d, $J = 7.7$ Hz), 5.87 (1H, q, $J = 6.6$ Hz), 4.81 (2H, s), 2.35 (2H, t, $J = 7.3$ Hz), 1.64–1.60 (2H, m), 1.54 (3H, d, $J = 6.6$ Hz), 1.27–1.24 (24H, m), 0.94 (9H, s), 0.86 (3H, t, $J = 6.6$ Hz), 0.10 (6H, s); ¹³C NMR (100 MHz, CDCl₃) δ 172.7, 160.8, 159.4, 137.1, 118.6, 117.9, 72.7, 65.9, 34.3, 31.8, 29.5, 29.4, 29.3, 29.2, 29.0, 29.0, 29.0, 25.7, 24.8, 22.5, 20.8, 18.1, 13.9, -5.6; HRMS (FAB) calcd for C₃₀H₅₆NO₃Si, MH⁺, 506.4030, found m/z 506.4045.

Preparation of S-23. **S-23** was obtained in 79% yield by desilylation of **S-29** with Bu₄NF. The synthetic method was the same as described for **S-25** except using EtOAc–hexane (3:7) as eluent for column chromatography: colorless crystals; mp 78–79 °C (hexane); $R_f = 0.22$ (EtOAc–hexane, 3:7); $[\alpha]_D^{25} -40.2$ (*c* 0.92, CHCl₃); IR (KBr) 3180, 1730 cm⁻¹; ¹H NMR (400 MHz, CDCl₃) δ 7.67 (1H, t, $J = 7.7$ Hz), 7.24 (1H, d, $J = 7.7$ Hz), 7.12 (1H, d, $J = 7.7$ Hz), 5.93 (1H, q, $J = 6.7$ Hz), 4.75 (2H, s), 3.92 (1H, br s), 2.38 (2H, t, $J = 6.8$ Hz), 1.68–1.61 (2H, m), 1.59 (3H, d, $J = 6.7$ Hz), 1.30–1.25 (24H, m), 0.88 (3H, t, $J = 7.0$ Hz); ¹³C NMR (100 MHz, CDCl₃) δ 173.0, 159.5,

158.4, 137.3, 119.2, 118.7, 72.5, 63.8, 34.5, 31.9, 29.7, 29.7, 29.6, 29.5, 29.4, 29.2, 29.1, 25.0, 22.7, 20.7, 14.1; HRMS (EI) calcd for $C_{24}H_{41}NO_3$, M^+ , 391.3087, found m/z 391.3100. Anal. Calcd for $C_{24}H_{41}NO_3$: C, 73.61; H, 10.55; N, 3.58. Found: C, 73.39; H, 10.63; N, 3.68.

Preparation of R-20. R-20 was obtained in 78% yield by tritylation of R-25 with trityl chloride. The synthetic method was the same as described for 15 except using EtOAc-hexane (3:7) as eluent for column chromatography: colorless oil; R_f = 0.33 (EtOAc-hexane, 3:7); $[\alpha]_D^{26}$ -1.57 (c 1.92, $CHCl_3$); IR (neat) 3410 cm^{-1} ; 1H NMR (300 MHz, $CDCl_3$) δ 7.75 (1H, t, J = 7.6 Hz), 7.68 (1H, dm, J = 7.6 Hz), 7.56-7.48 (6H, m), 7.36-7.20 (9H, m), 7.12 (1H, dm, J = 7.6 Hz), 4.81 (1H, qd, J = 6.6 and 4.4 Hz), 4.42 (1H, d, J = 4.4 Hz), 4.34 (2H, s), 1.45 (3H, d, J = 6.6 Hz); ^{13}C NMR (75 MHz, $CDCl_3$) δ 161.7, 157.7, 143.7, 137.4, 128.6, 127.9, 127.1, 119.1, 117.9, 87.1, 68.3, 66.6, 24.2; HRMS (FAB) calcd for $C_{27}H_{26}NO_2$, MH^+ , 396.1964, found m/z 396.1966.

Extraction Experiments. Extraction experiments were carried out by adding a CH_2Cl_2 solution of the podand (0.015 mmol, 1.5 mL) to an aqueous solution of six metal perchlorates (0.015 mmol each, 1.5 mL). After the mixture had been stirred for 2 h, the aqueous phase was separated. The concentrations of metal cations were determined by atomic absorption or flame spectroscopy (performed at Exlan Technical Center Co., Okayama) and used to calculate the extraction percentage and apparent extraction equilibrium constant K_{ex} (L/mol).

Transport Experiments. Transport experiments were performed at room temperature (ca. 20 °C) in a U-tube glass cell (2.0-cm i.d.).¹⁷ The carrier, dissolved in CH_2Cl_2 , was placed in the base of the U-tube, and the two aqueous phases were placed in the tube arms, floating on the membrane phase. The membrane phase was stirred constantly with a magnetic stirrer. The transport rates listed in Table 3 were calculated from the initial rates of appearance of metal cation into the

aqueous receiving phase, which were determined spectroscopically (at Exlan Technical Center Co., Okayama). We confirmed that no metal salt was transported in the absence of carrier (transport rate $< 0.3 \times 10^{-6}$ mol/h).

NMR Studies of Ag^+ Binding. ^{13}C NMR binding experiments were carried out with a JEOL 90 A spectrometer. Each podand was dissolved in $CDCl_3$ - CH_3OH (4:1) at a concentration of 0.05 mol/L.

Computational Method. The calculations were carried out using Spartan SGI version 4.0.1 (*ab initio*, STO-3G). Acyclic podands are generally flexible so it is very difficult to search all of the stationary points of their geometries and obtain global minima for their structures. We made initial geometries of complexed podands on the basis of semiempirical calculations. Due to a lack of a parameter for Ag^+ , Li^+ complexes were first optimized using the Spartan PM3 program. The geometries obtained were adopted as the starting structures for optimization. The metal cation of the Li^+ complex was replaced with Ag^+ to provide a starting structure for the Ag^+ complex. Although we determined the parameters for Ag^+ for calculations *via an ab initio* method, we could not estimate quantitative stabilization energies due to the complex formation. However we did obtain qualitative insight into the effect of ligand geometry and stereochemically controlled substitution on Ag^+ binding by the podand.

Acknowledgment. This research was supported in part by Grant-in-Aids for Scientific Research (Nos. 08454205 and 09238249) from the Ministry of Education, Science, Sports and Culture, Japan.

Supporting Information Available: ^{13}C NMR spectra of compounds lacking elemental analyses (35 pages). This material is contained in libraries on microfiche, immediately follows this article in the microfilm version of the journal, and can be ordered from the ACS; see any current masthead page for ordering information.

(17) Tsukube, H. In *Liquid Membrane: Chemical Applications*; Araki, T., Tsukube, H., Eds.; CRC Press: Boca Raton, FL, 1990; pp 20-50.